

Spectral shift, electronic coupling and exciton delocalization in nanocrystal dimers: insights from all-atom electronic structure computations

Maurizio Coden, Pietro De Checchi, Barbara Fresch*

Dipartimento di Scienze Chimiche, Università degli Studi di Padova, Via Marzolo 1, 35131 Padova, Italy.

Supporting information

Index

1. Benchmark of computational protocol	3
2. Formal definition of the participation ratio (PR) and charge transfer (CT) indexes.....	6
3. Details on the electronic structure of ($\text{Cd}_{13}\text{Se}_{13}$)-PDTC-($\text{Cd}_{13}\text{Se}_{13}$)	9
3.1. Density of states of monomer ($\text{Cd}_{13}\text{Se}_{13}$)-PDTC and dimer ($\text{Cd}_{13}\text{Se}_{13}$)-PDTC.....	9
3.2. Simulated spectra of monomer ($\text{Cd}_{13}\text{Se}_{13}$)-PDTC and dimer of ($\text{Cd}_{13}\text{Se}_{13}$)-PDTC-($\text{Cd}_{13}\text{Se}_{13}$).....	9
3.3. Frontier orbitals of monomer ($\text{Cd}_{13}\text{Se}_{13}$)-PDTC	10
3.4. Selected Natural Transition Orbitals for ($\text{Cd}_{13}\text{Se}_{13}$)-PDTC	11
3.5. Frontier orbitals of dimer ($\text{Cd}_{13}\text{Se}_{13}$)-PDTC-($\text{Cd}_{13}\text{Se}_{13}$)	12
4. Details on the electronic structure of ($\text{Cd}_{13}\text{Se}_{13}$)-propanDTC-($\text{Cd}_{13}\text{Se}_{13}$)	14
4.1. Density of states of monomer ($\text{Cd}_{13}\text{Se}_{13}$)-propanDTC and dimer of ($\text{Cd}_{13}\text{Se}_{13}$)-propanDTC-($\text{Cd}_{13}\text{Se}_{13}$).	14
4.2. simulated spectra of monomer ($\text{Cd}_{13}\text{Se}_{13}$)-propanDTC and dimer of ($\text{Cd}_{13}\text{Se}_{13}$)-propanDTC-($\text{Cd}_{13}\text{Se}_{13}$)	14
4.3. Natural transition orbitals of monomer ($\text{Cd}_{13}\text{Se}_{13}$)-propan DTC	15
4.4. Natural transition orbitals of dimer ($\text{Cd}_{13}\text{Se}_{13}$)-propanDTC-($\text{Cd}_{13}\text{Se}_{13}$)	16
5. Comparison between PDTC and propan-DTC.....	17
6. Details on the electronic structure of ($\text{Cd}_{13}\text{Se}_{13}$)-BTT-($\text{Cd}_{13}\text{Se}_{13}$)	18
6.1. Density of states of monomer ($\text{Cd}_{13}\text{Se}_{13}$)-BTT and dimer of ($\text{Cd}_{13}\text{Se}_{13}$)-BTT-($\text{Cd}_{13}\text{Se}_{13}$)	18
6.2. Simulated spectra of monomer ($\text{Cd}_{13}\text{Se}_{13}$)-BTT and dimer of ($\text{Cd}_{13}\text{Se}_{13}$)-BTT-($\text{Cd}_{13}\text{Se}_{13}$)	18
6.3. Natural transition orbitals monomer ($\text{Cd}_{13}\text{Se}_{13}$)-BTT.....	19
6.4. Natural transition orbitals of dimer of ($\text{Cd}_{13}\text{Se}_{13}$)-BTT-($\text{Cd}_{13}\text{Se}_{13}$)	20
7. Details on the electronic structure of ($\text{Cd}_{13}\text{Se}_{13}$)-NTT-($\text{Cd}_{13}\text{Se}_{13}$).....	22
7.1. Density of states of monomer ($\text{Cd}_{13}\text{Se}_{13}$)-NTT and dimer of ($\text{Cd}_{13}\text{Se}_{13}$)-NTT-($\text{Cd}_{13}\text{Se}_{13}$)	22
7.2. Simulated spetra of monomer ($\text{Cd}_{13}\text{Se}_{13}$)-NTT and dimer of ($\text{Cd}_{13}\text{Se}_{13}$)-NTT-($\text{Cd}_{13}\text{Se}_{13}$).....	22
7.3. Frontier Orbitals of monomer ($\text{Cd}_{13}\text{Se}_{13}$)-NTT	23
7.4. Natural transition orbitals of monomer ($\text{Cd}_{13}\text{Se}_{13}$)-NTT	23

7.5.	Frontier orbitals of dimer ($\text{Cd}_{13}\text{Se}_{13}$)-NTT-($\text{Cd}_{13}\text{Se}_{13}$)	24
7.6.	Natural transition orbitals of dimer ($\text{Cd}_{13}\text{Se}_{13}$)-NTT-($\text{Cd}_{13}\text{Se}_{13}$).....	25
8.	Comparison between BTT and NTT	27
9.	Details on the electronic structure of $\text{Cd}_{17}\text{Se}_4(\text{SCH}_3)_{26}$ -Py-Py- $\text{Cd}_{17}\text{Se}_4(\text{SCH}_3)_{26}$	28
9.1.	Density of states of monomer $\text{Cd}_{17}\text{Se}_4(\text{SCH}_3)_{26}$ -Py and dimer $\text{Cd}_{17}\text{Se}_4(\text{SCH}_3)_{26}$ -Py-Py- $\text{Cd}_{17}\text{Se}_4(\text{SCH}_3)_{26}$.	28
9.2.	Simulated spectra of monomer $\text{Cd}_{17}\text{Se}_4(\text{SCH}_3)_{26}$ -Py	28
9.3.	Natural transition orbitals of monomer $\text{Cd}_{17}\text{Se}_4(\text{SCH}_3)_{26}$ -Py.....	29
9.4.	Simulated spectra of dimer $\text{Cd}_{17}\text{Se}_4(\text{SCH}_3)_{26}$ -Py-Py- $\text{Cd}_{17}\text{Se}_4(\text{SCH}_3)_{26}$	30
9.5.	Natural transition orbitals of dimer $\text{Cd}_{17}\text{Se}_4(\text{SCH}_3)_{26}$ -Py-Py- $\text{Cd}_{17}\text{Se}_4(\text{SCH}_3)_{26}$	31
10.	Structures, distances and coupling.....	33
11.	Optimized Coordinates.....	35
11.1.	$\text{Cd}_{13}\text{Se}_{13}$ -PDTC- $\text{Cd}_{13}\text{Se}_{13}$	35
11.2.	$\text{Cd}_{13}\text{Se}_{13}$ -BTT- $\text{Cd}_{13}\text{Se}_{13}$	36
11.3.	$\text{Cd}_{17}\text{Se}_4(\text{SCH}_3)_{26}$ -Py-Py- $\text{Cd}_{17}\text{Se}_4(\text{SCH}_3)_{26}$	37
12.	References	41

1. Benchmark of computational protocol

To set up a predictive computational protocol we benchmark different functionals against experimental results for a smaller cluster whose composition is very similar to the dimers showed in Figure 1 of the main text. We selected an atomically well-defined CdSe cluster that was experimentally isolated and structurally characterized. The cluster $\text{Cd}_{10}\text{Se}_4(\text{SePh})_{12}(\text{PPh}_3)_4$, hereafter **Cd10**, can be prepared through a selective synthetic route, single crystal structure is available¹ and the absorption spectrum has been characterized.² Importantly for our purpose, it can be modelled at the DFT level without introducing major structural simplification allowing a straightforward comparison of the computed spectra with the experimental one. The structure of **Cd10** is shown in Figure S1 a). Absorption spectra were calculated using TDDFT and CIS (Configuration interaction singles). A total of 120 singlet transitions were included in the excited state calculations to represent absorption spectra up to 4.5-5 eV. The optical transitions were in turn broadened by a Gaussian function with a line width of 80 meV. Figure S1 b) shows the experimental absorption spectrum taken from ref ² (black line) compared with the absorption spectra obtained with 7 different hybrid functionals as reported in the legend together with the shift (in eV) of the predicted first band compared to the experimental position. Absolute transition energies are well described by the recent functional from Truhlar group MN15³ (green line) while they are systematically overestimated by long range corrected functionals such as CAMB3LYP and wB97XD. However, because we are interested in relative energies of excited states more than absolute energies, we also compare the calculated absorption profile shifted by the difference in the first transition band (Figure S1 c). In this case, CAMB3LYP gives the best description of the relative intensities of different bands. Corrections in the functional form of the long-range part of the exchange interaction are also expected to better describe high energy excited states, the interactions between the cores separated by the linker and state with charge transfer character.⁴

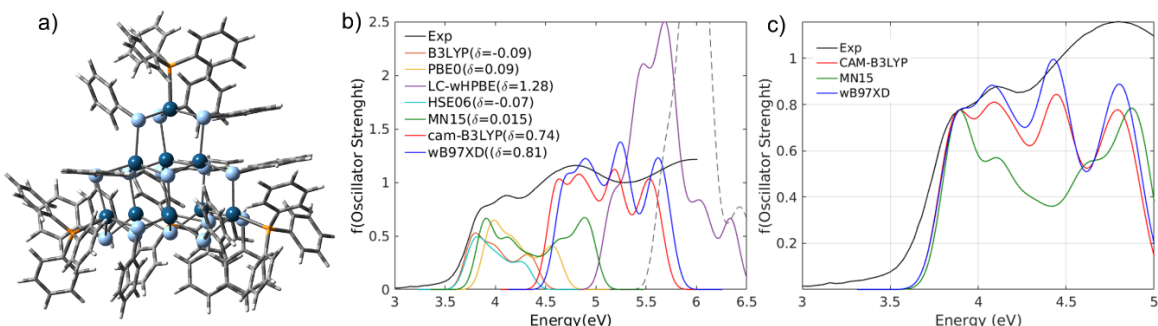


Figure S1: a) optimized geometry of Cd10. b) Experimental absorption spectrum (black line) and spectra calculated with different functionals as detailed in the legend. Values in parenthesis are the shift in eV of the position of the first band compared to the experimental value. Dashed line is the CIS spectrum. B3LYP, PBE0, HSE06, MN15 are hybrid functionals (which include a mixture of Hartree-Fock exchange with DFT exchange-correlation). CAM-B3LYP, wB97XD and LC-wHPBE are long range corrected hybrid functionals. c) Spectra of three selected functionals as specified in the legend shifted to ease comparison with the experimental spectrum (black).

The effect of the substitution of Phenil (Ph) with metil (Me) groups in a fully covered cluster has been investigated for **Cd10**. Figure S2 shows the comparison between $\text{Cd}_{10}\text{Se}_4(\text{SePh})_{12}(\text{PPh}_3)_4$ (blue) and $\text{Cd}_{10}\text{Se}_4(\text{SeMe})_{12}(\text{PMMe}_3)_4$ (red) simulated spectra. In the first band, a slight blue shift can be noticed together with a narrowing of the band moving from phenyl to methyl groups. However, NTOs analysis (shown in Figure S3 for selected transitions) evidences a strong similarity in the nature of the first band transitions. The electron is mainly localized in s-orbital of Cd while p-orbitals of Se provide the major contribution to the hole. In $\text{Cd}_{10}\text{Se}_4(\text{SePh})_{12}(\text{PPh}_3)_4$ phenil rings partially delocalizes the hole, nevertheless the spatial localization of holes and electrons does not change

substantially. These results suggest that the substitution of phenyl with methyl groups does not change the nature of the excited states while providing a great advantage in term of computational efficiency.

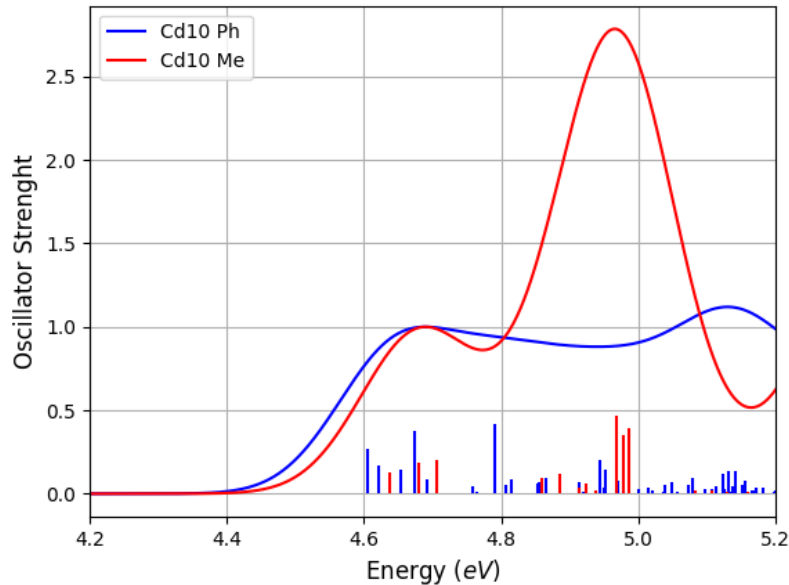


Figure S2: Normalized spectra of $\text{Cd}_{10}\text{Se}_4(\text{SePh})_{12}(\text{PPh}_3)_4$ (blue) and $\text{Cd}_{10}\text{Se}_4(\text{SeMe})_{12}(\text{PMe}_3)_4$ (red) obtained using cam-b3lyp functional, lanl2dz basis set for Cd and Se atoms and 6-31g(d) for C, H and P atoms.

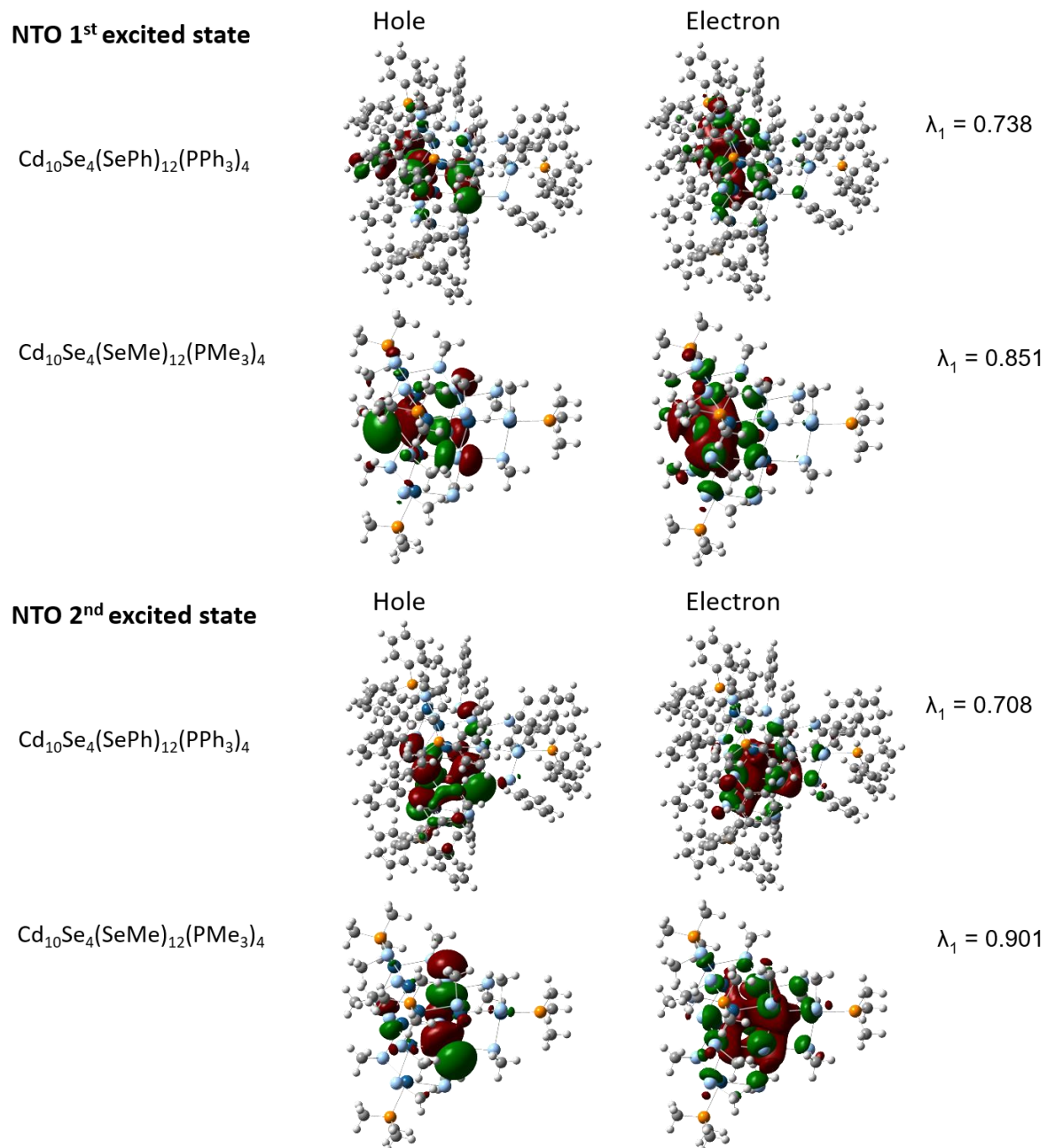


Figure S3: Natural transition orbitals of the first two transition for Cd10Se4(SePh)12(PPh3)4 and Cd10Se4(SeMe)12(PMe3)4, together with their singular value

2. Formal definition of the participation ratio (PR) and charge transfer (CT) indexes

The analysis is based on the one-particle transition density matrix⁵ which describes the electronic excitation between the ground state $|\Psi_0\rangle$ and the electronically excited state $|\Psi_E\rangle$

$$\rho_{pq}^{0E} = \langle \Psi_0 | \hat{p}^\dagger \hat{q} | \Psi_E \rangle \quad (1)$$

where \hat{p}^\dagger and \hat{q} are the (spin averaged) creation and annihilation operators of the orbitals p and q . Following Ref.⁶ let us first consider the simplest case of two systems, A and B, each characterized by two active orbitals, a HOMO ground state (g) orbital and a LUMO virtual orbital (e), which may interact to form a dimer. In the ground state both g_A and g_B are doubly occupied while e_A and e_B are empty. By considering single excitations from the ground state, four excited states can be built

$$|\Psi_{g_A \rightarrow e_A}\rangle = \frac{1}{\sqrt{2}} e_A^\dagger g_A |\Psi_0\rangle \quad |\Psi_{g_B \rightarrow e_B}\rangle = \frac{1}{\sqrt{2}} e_B^\dagger g_B |\Psi_0\rangle$$

$$|\Psi_{g_B \rightarrow e_A}\rangle = \frac{1}{\sqrt{2}} e_A^\dagger g_B |\Psi_0\rangle \quad |\Psi_{g_A \rightarrow e_B}\rangle = \frac{1}{\sqrt{2}} e_B^\dagger g_A |\Psi_0\rangle$$

The two states in the first row corresponds to excitation where both the hole and the electron are localized in the same fragment, while the states in the second row describe charge transfer (CT) states where an electron from the HOMO of one fragment is excited to the LUMO of the other fragment. These states are showed in figure S1 in the localized basis. In an ideal homodimer, the localized excitation and the CT are pairwise degenerated, leading to delocalized eigenfunctions: two excitonic resonance states and two charge resonance states showed in the second row of figure S1.

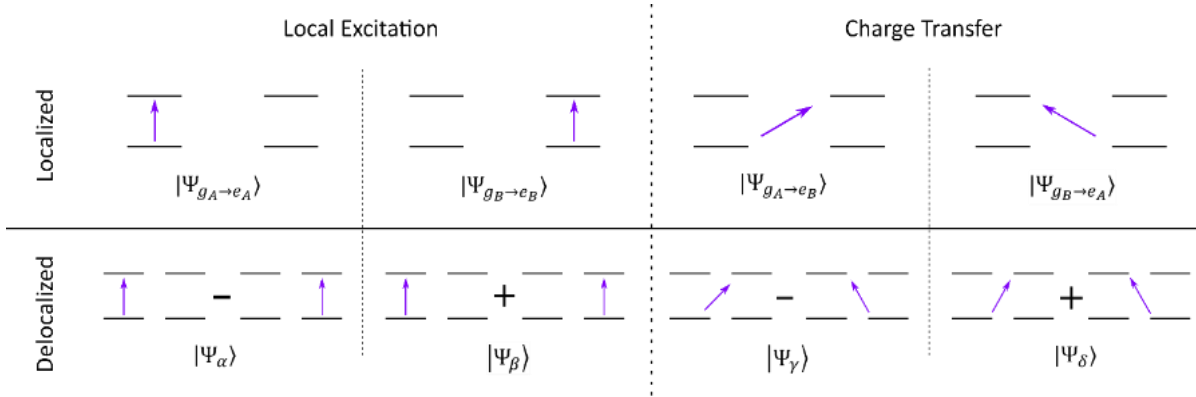


Figure S3: Schematic representation of excited states in an ideal homodimer. On the left excitations where the initial and final orbitals are located on the same system, on the right the charge transfer states. The top panels represent localized excitations while, in the bottom panels, their linear combination are delocalized states.

Based on the transition density matrix corresponding to an electronic excited state we now introduce two indexes which are able to quantify the charge transfer character and the delocalization of the exciton. The transition density matrix, Eq.(1), of the states shown in figure 3 in the local basis (g_A, e_A, g_B, e_B) are reported in Table 1.

State	$ \Psi_{g_A \rightarrow e_A}\rangle$	$ \Psi_{g_B \rightarrow e_B}\rangle$	$ \Psi_{g_B \rightarrow e_A}\rangle$	$ \Psi_{g_A \rightarrow e_B}\rangle$
$\hat{\rho}^{0E}$	$\begin{pmatrix} 0 & \sqrt{2} & 0 & 0 \\ 0 & 0 & 0 & 0 \\ 0 & 0 & 0 & 0 \\ 0 & 0 & 0 & 0 \end{pmatrix}$	$\begin{pmatrix} 0 & 0 & 0 & 0 \\ 0 & 0 & 0 & 0 \\ 0 & 0 & 0 & \sqrt{2} \\ 0 & 0 & 0 & 0 \end{pmatrix}$	$\begin{pmatrix} 0 & 0 & 0 & 0 \\ 0 & 0 & 0 & 0 \\ 0 & \sqrt{2} & 0 & 0 \\ 0 & 0 & 0 & 0 \end{pmatrix}$	$\begin{pmatrix} 0 & 0 & 0 & \sqrt{2} \\ 0 & 0 & 0 & 0 \\ 0 & 0 & 0 & 0 \\ 0 & 0 & 0 & 0 \end{pmatrix}$
Ω^{0E}	$\begin{pmatrix} 1 & 0 \\ 0 & 0 \end{pmatrix}$	$\begin{pmatrix} 0 & 0 \\ 0 & 1 \end{pmatrix}$	$\begin{pmatrix} 0 & 0 \\ 1 & 0 \end{pmatrix}$	$\begin{pmatrix} 0 & 1 \\ 0 & 0 \end{pmatrix}$
CT	0	0	1	1
PR	1	1	1	1
PR_{NTO}	1	1	1	1

State	$ \psi_\alpha\rangle$	$ \psi_\beta\rangle$	$ \psi_\gamma\rangle$	$ \psi_\delta\rangle$
$\hat{\rho}^{0E}$	$\begin{pmatrix} 0 & 1 & 0 & 0 \\ 0 & 0 & 0 & 0 \\ 0 & 0 & 0 & -1 \\ 0 & 0 & 0 & 0 \end{pmatrix}$	$\begin{pmatrix} 0 & 1 & 0 & 0 \\ 0 & 0 & 0 & 0 \\ 0 & 0 & 0 & 1 \\ 0 & 0 & 0 & 0 \end{pmatrix}$	$\begin{pmatrix} 0 & 0 & 0 & -1 \\ 0 & 0 & 0 & 0 \\ 0 & 1 & 0 & 0 \\ 0 & 0 & 0 & 0 \end{pmatrix}$	$\begin{pmatrix} 0 & 0 & 0 & 1 \\ 0 & 0 & 0 & 0 \\ 0 & 1 & 0 & 0 \\ 0 & 0 & 0 & 0 \end{pmatrix}$
Ω^{0E}	$\begin{pmatrix} 0.5 & 0 \\ 0 & 0.5 \end{pmatrix}$	$\begin{pmatrix} 0.5 & 0 \\ 0 & 0.5 \end{pmatrix}$	$\begin{pmatrix} 0 & 0.5 \\ 0.5 & 0 \end{pmatrix}$	$\begin{pmatrix} 0 & 0.5 \\ 0.5 & 0 \end{pmatrix}$
CT	0	0	1	1
PR	2	2	2	2
PR_{NTO}	2	2	2	2

Table S1 Transition density matrix $\hat{\rho}^{0E}$ represented in local basis (g_A, e_A, g_B, e_B); matrix of charge transfer numbers Ω^{0E} ; Charge Transfer index (CT); participation ratio (PR) and participation ratio of NTO (PR_{NTO}). The table on top refers to locally excited states $|\Psi_{g_A \rightarrow e_A}\rangle$ and $|\Psi_{g_B \rightarrow e_B}\rangle$ and charge transfer states $|\Psi_{g_B \rightarrow e_A}\rangle$, $|\Psi_{g_A \rightarrow e_B}\rangle$. The bottom table refers to excitonic resonant states $|\Psi_\alpha\rangle$ and $|\Psi_\beta\rangle$ and charge resonance states $|\Psi_\gamma\rangle$, $|\Psi_\delta\rangle$.

The transition densities for states composed of local excitations have non-zero elements on the diagonal blocks while states containing charge-transfer configurations have non-zero elements in the off-diagonal blocks. From this consideration, a charge transfer number Ω_{AB}^{0E} has been defined as the summation of the transition density matrix elements

$$\Omega_{AB}^{0E} = \sum_{\substack{a \in A \\ b \in B}} (\rho_{ab}^{0E})^2$$

where A and B index the two fragments. If $A=B$ then a and b are orbitals localized on the same fragment and $\Omega_{AA}, \Omega_{BB} \neq 0$ are the weights of local excitations. For charge transfer contributions, orbitals a and b are in different fragments and $\Omega_{AB}, \Omega_{BA} \neq 0$. A one-value index reflecting the charge transfer character (CT) is defined as

$$CT = \frac{1}{\Omega} \sum_{\substack{A \\ B \neq A}} \Omega_{AB}$$

Where the normalization factor is $\Omega = \sum_{A,B} \Omega_{AB}$ is exactly 1 for a normalized CIS wave function, while is very close to one for states mainly described by a single electron transition. The CT index describes the total amount of configurations where the orbitals in the initial and in the final state belong to different fragments. It assumes value of 1 if the excitation is a net charge transfer while is 0 when the excitation is purely local, see e.g. Table 1.

The general formulation for non-orthogonal atomic orbitals has been proposed and developed by Plasser et. al⁶,⁷ and can be applied to the TDDFT formalism.

Another index quantifies the *degree of delocalization* of the excited state amongst different fragments. The participation ratio (PR) reflects the number of fragments participating to the initial and final states involved in the excitation

$$PR = \frac{1}{2} \left(\frac{\Omega^2}{\sum_A (\sum_B \Omega_{AB})^2} + \frac{\Omega^2}{\sum_B (\sum_A \Omega_{AB})^2} \right)$$

where the sum in parenthesis of the first term considers all the configurations where the initial orbital is localized on the specific fragment A and goes over any possible fragments B. The first term quantifies the delocalization of the *hole* while the second term refers to the *electron*. For the states of figure 3, PR=1 for the state involving completely localized hole and electron states while PR=2 for the resonant excitonic and CT states.

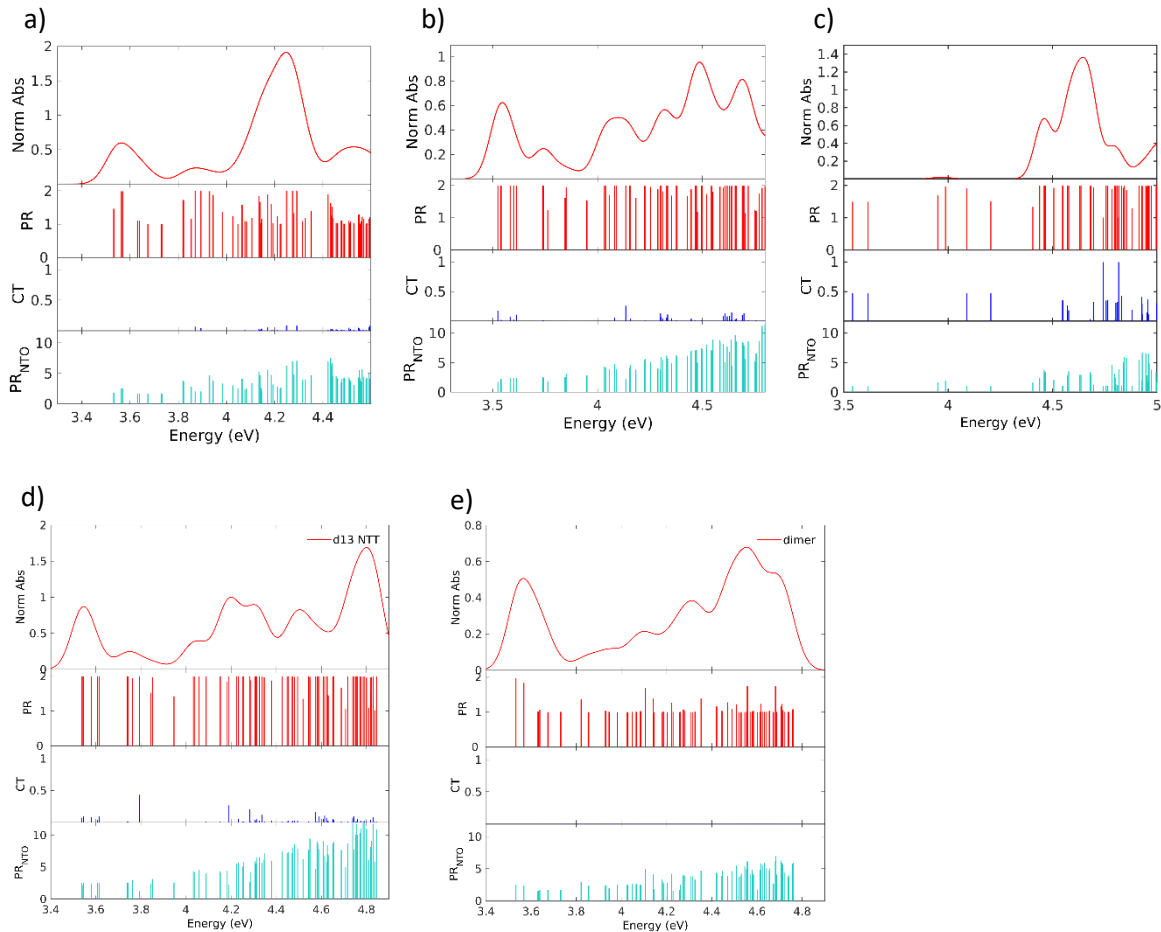


Figure S4: Top panels show simulated absorption spectra by broadened gaussian functions for each transition. Panels below report PR, CT and PR_{NTO}, each bar represent an excited states. a) (Cd₁₃Se₁₃) -PDTC-(Cd₁₃Se₁₃) system, gaussian broadening $\sigma=0.05$ eV; b) (Cd₁₃Se₁₃) -BTT-(Cd₁₃Se₁₃) with $\sigma=0.05$ eV; c) Cd₁₇Se₄(SCH₃)₂₆-Py-Py- Cd₁₇Se₄(SCH₃)₂₆ system and $\sigma=0.04$ eV, d) (Cd₁₃Se₁₃) -NTT-(Cd₁₃Se₁₃) system, gaussian broadening $\sigma=0.05$ eV; e) (Cd₁₃Se₁₃) -propanDTC-(Cd₁₃Se₁₃) with $\sigma=0.05$ eV.

3. Details on the electronic structure of $(\text{Cd}_{13}\text{Se}_{13})$ -PDTC- $(\text{Cd}_{13}\text{Se}_{13})$

3.1. Density of states of monomer $(\text{Cd}_{13}\text{Se}_{13})$ -PDTC and dimer $(\text{Cd}_{13}\text{Se}_{13})$ -PDTC

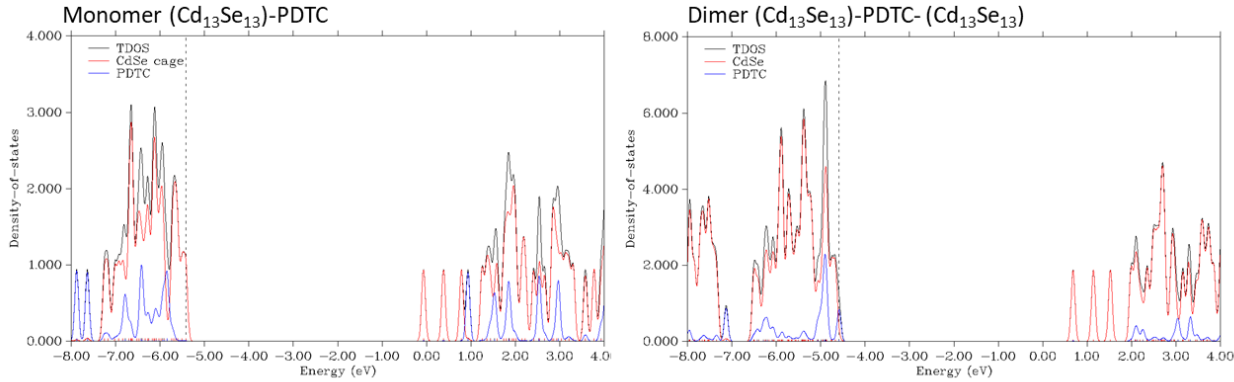


Figure S5: Projected density of states for monomer $(\text{Cd}_{13}\text{Se}_{13})$ -PDTC (left) and for dimer $(\text{Cd}_{13}\text{Se}_{13})$ -PDTC- $(\text{Cd}_{13}\text{Se}_{13})$ (right), obtained with Mulliken scheme (FWHM=0.1eV). PDTC ligand states reported in blue and $\text{Cd}_{13}\text{Se}_{13}$ states in red. Black line represents the total density of states (TDOS).

3.2. Simulated spectra of monomer $(\text{Cd}_{13}\text{Se}_{13})$ -PDTC and dimer of $(\text{Cd}_{13}\text{Se}_{13})$ -PDTC- $(\text{Cd}_{13}\text{Se}_{13})$

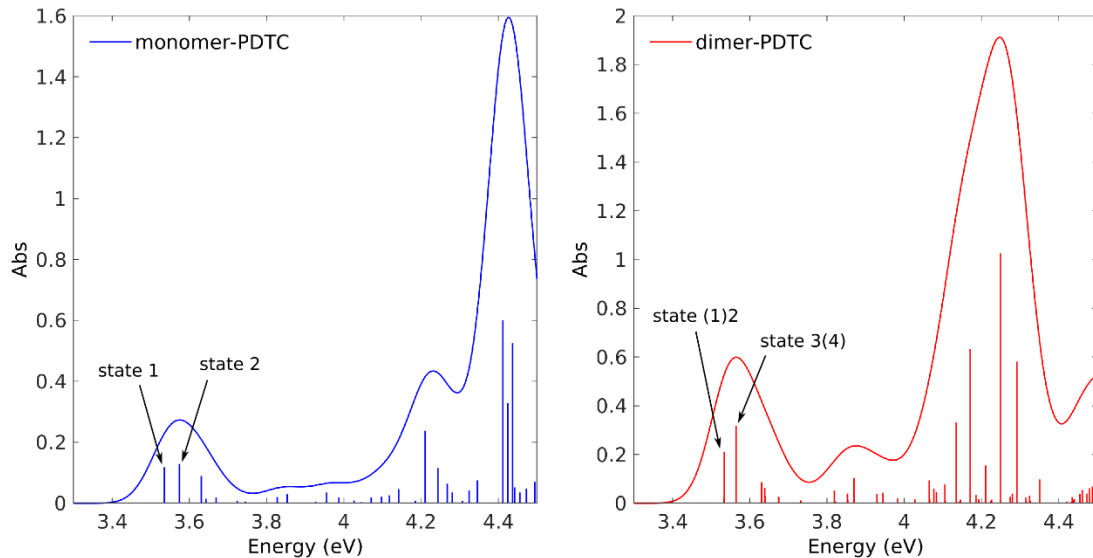


Figure S6: Simulated absorption spectra ($\sigma=0.05\text{eV}$) of monomer $(\text{Cd}_{13}\text{Se}_{13})$ -PDTC (left, blue) and of dimer $(\text{Cd}_{13}\text{Se}_{13})$ -PDTC- $(\text{Cd}_{13}\text{Se}_{13})$ (right, red). First excited states are progressively numbered. Between parentheses, the excited states with low oscillator strength, difficult to pinpoint by eye, are reported.

3.3. Frontier orbitals of monomer ($\text{Cd}_{13}\text{Se}_{13}$)-PDTC

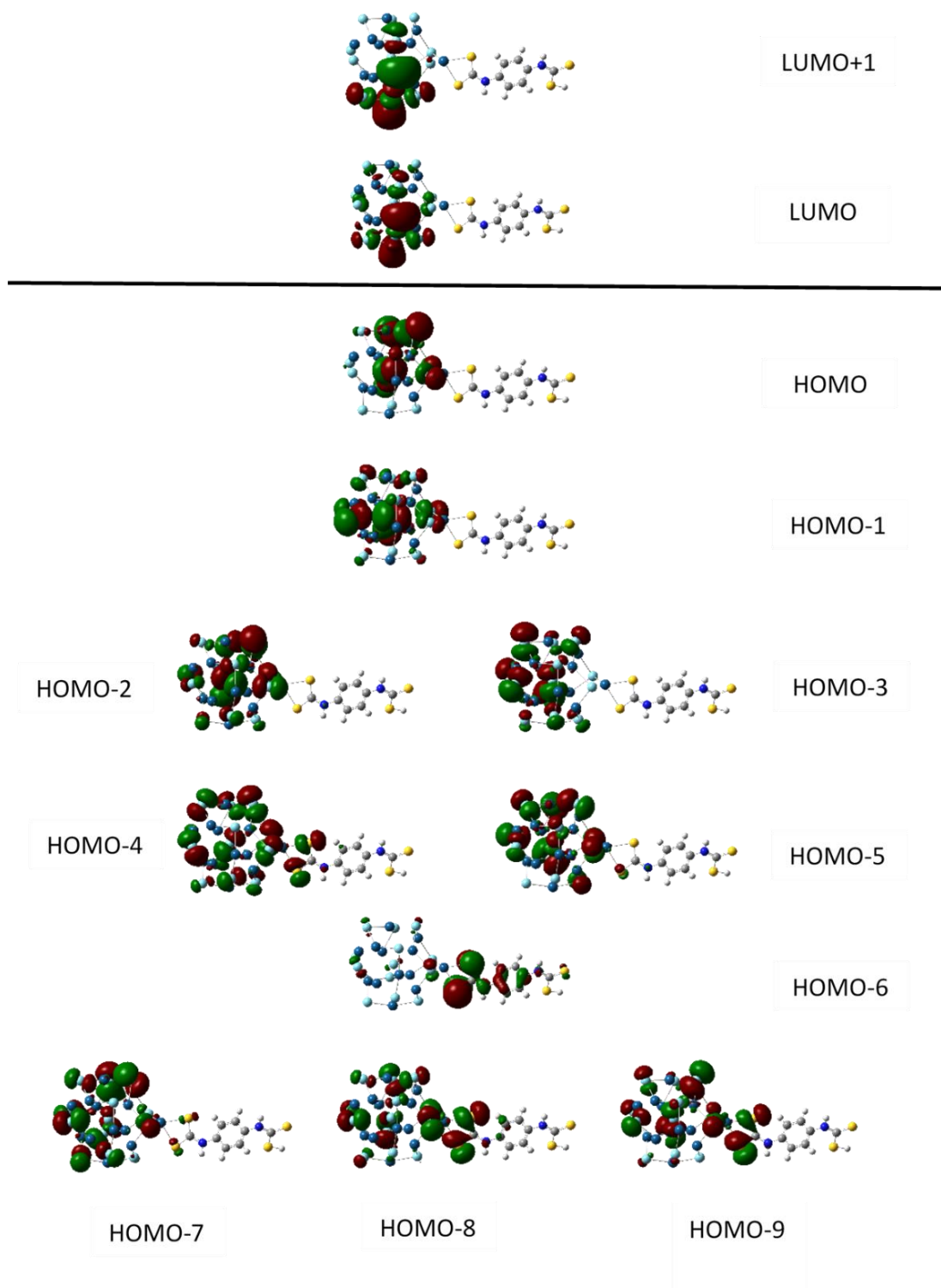
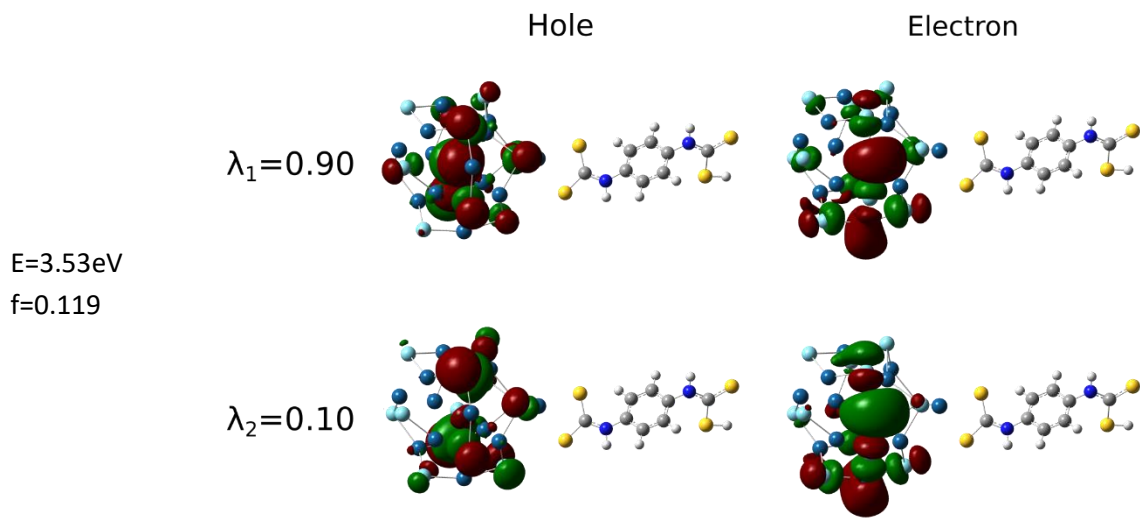


Figure S7: Monomer ($\text{Cd}_{13}\text{Se}_{13}$)-PDTC representative frontier orbitals are reported as level scheme. Orbitals placed side by side differ in energy less than 45meV.

3.4. Selected Natural Transition Orbitals for (Cd₁₃Se₁₃)-PDTC

NTO 1st excited state



NTO 2nd excited state

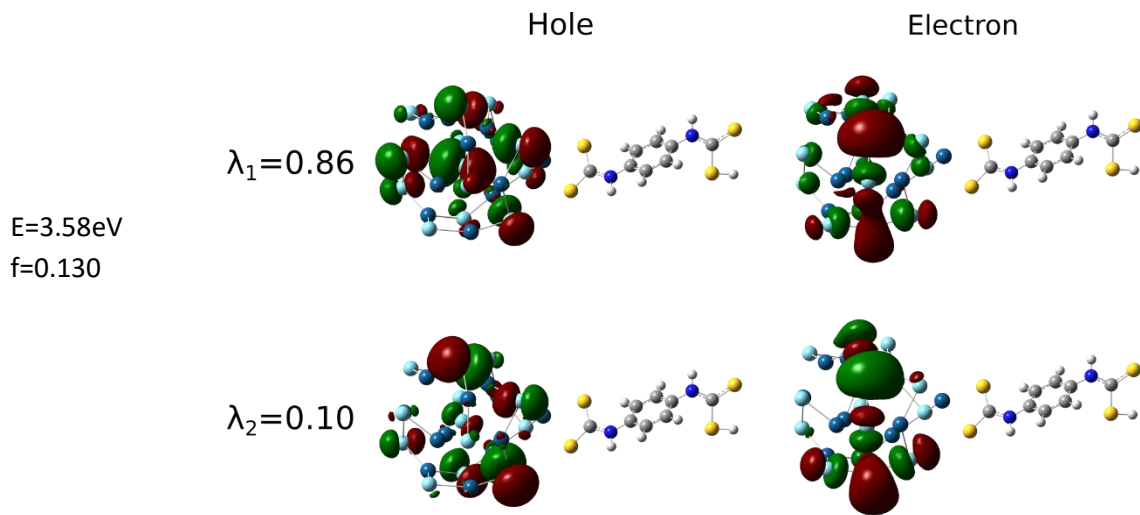


Figure S8: for the first two excited states excitation energy (E), oscillator strength (f) and Natural Transition orbitals (NTOs) with their singular values (λ_i) are reported.

3.5. Frontier orbitals of dimer ($\text{Cd}_{13}\text{Se}_{13}$)-PDTC-($\text{Cd}_{13}\text{Se}_{13}$)

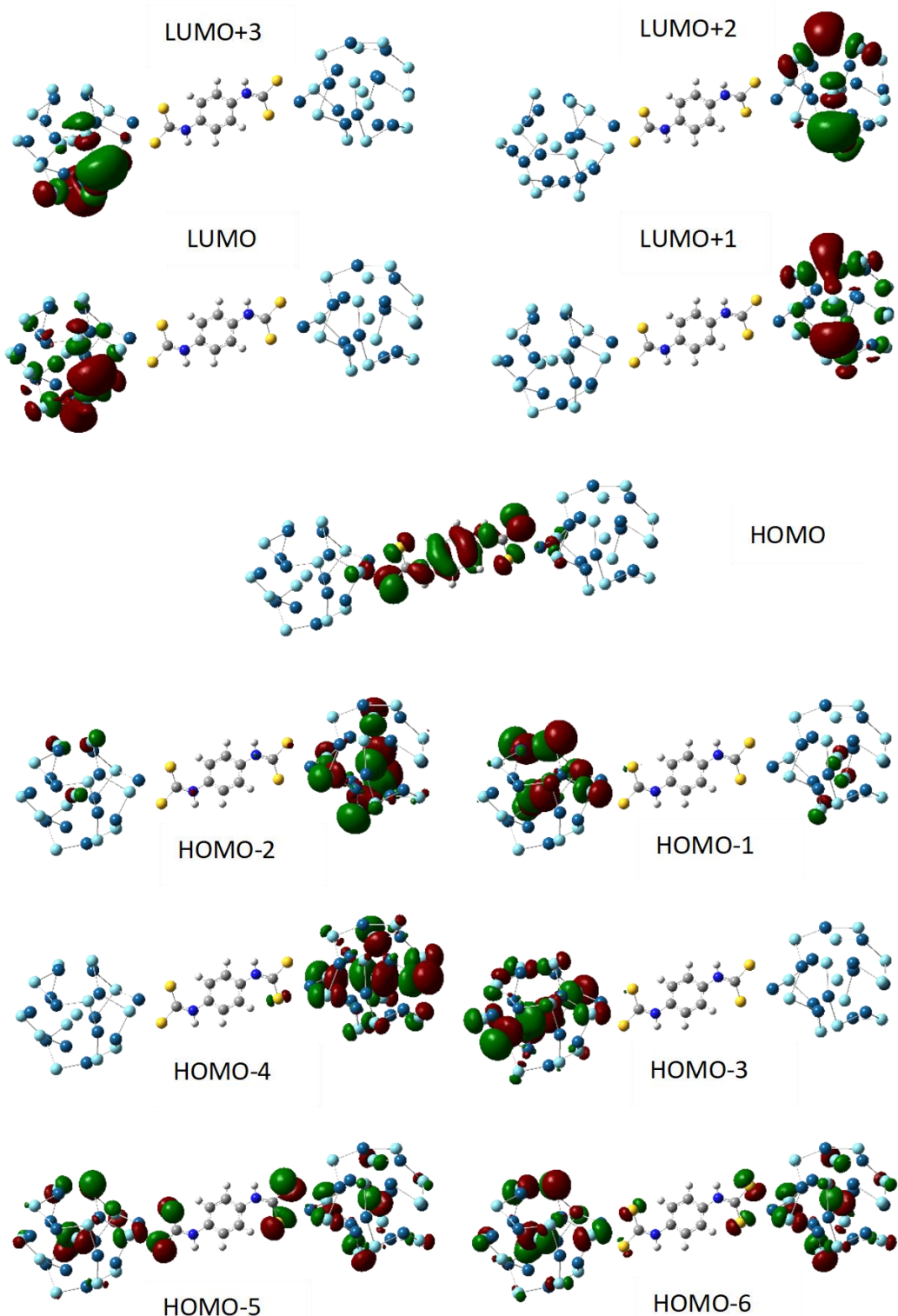
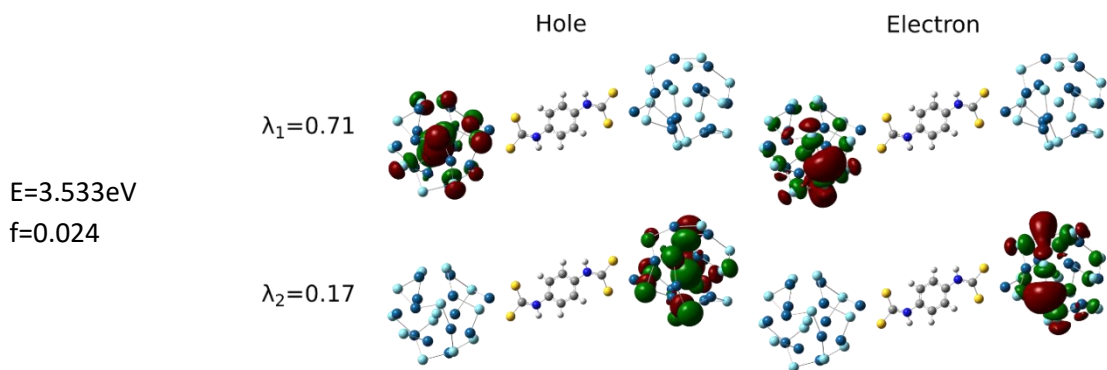


Figure S9: Dimer ($\text{Cd}_{13}\text{Se}_{13}$)-PDTC-($\text{Cd}_{13}\text{Se}_{13}$) representative frontiers orbitals reported as level scheme.

3.6. Selected Natural transition orbitals of dimer ($\text{Cd}_{13}\text{Se}_{13}$)-PDTC-($\text{Cd}_{13}\text{Se}_{13}$)

NTO 1st excited state

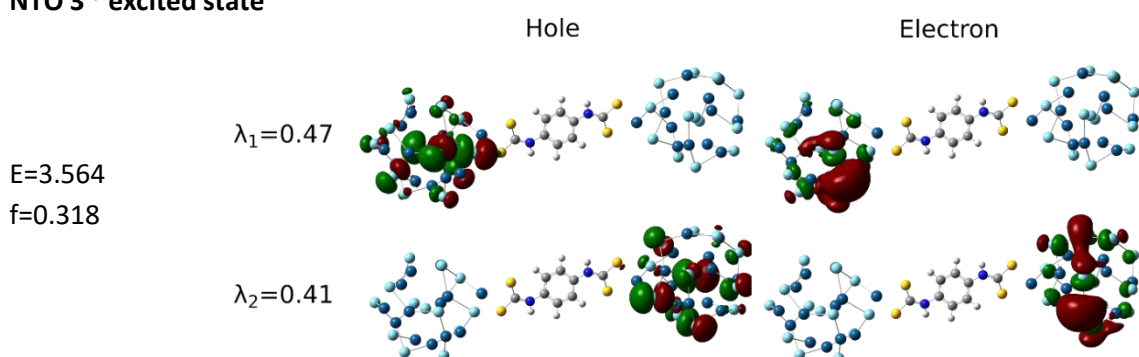


NTO 2nd excited state

E=3.534eV
f=0.218

Not reported
(same shape of 1st excitation NTOs with exchanged singular values $\lambda_1 \leftrightarrow \lambda_2$)

NTO 3rd excited state



NTO 4th excited state

$$\begin{aligned}E &= 3.569 \\f &= 0.0013\end{aligned}$$

Not reported
(same shape of 3rd excitation NTOs with exchanged singular values $\lambda_1 \leftrightarrow \lambda_2$)

NTO 5th excited state

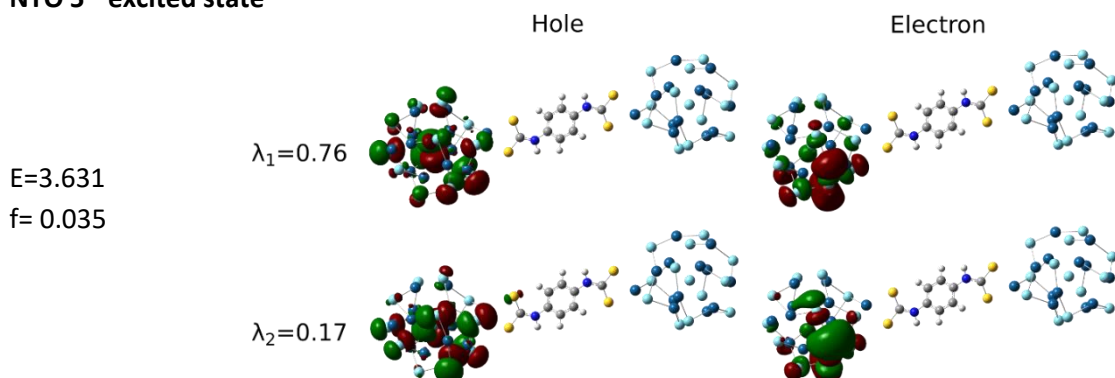


Figure S10: NTOs of representative low-energy excites states of dimer ($\text{Cd}_{13}\text{Se}_{13}$)-PDTC-($\text{Cd}_{13}\text{Se}_{13}$).

4. Details on the electronic structure of ($\text{Cd}_{13}\text{Se}_{13}$)-propanDTC-($\text{Cd}_{13}\text{Se}_{13}$)

4.1. Density of states of monomer ($\text{Cd}_{13}\text{Se}_{13}$)-propanDTC and dimer of ($\text{Cd}_{13}\text{Se}_{13}$)-propanDTC-($\text{Cd}_{13}\text{Se}_{13}$)

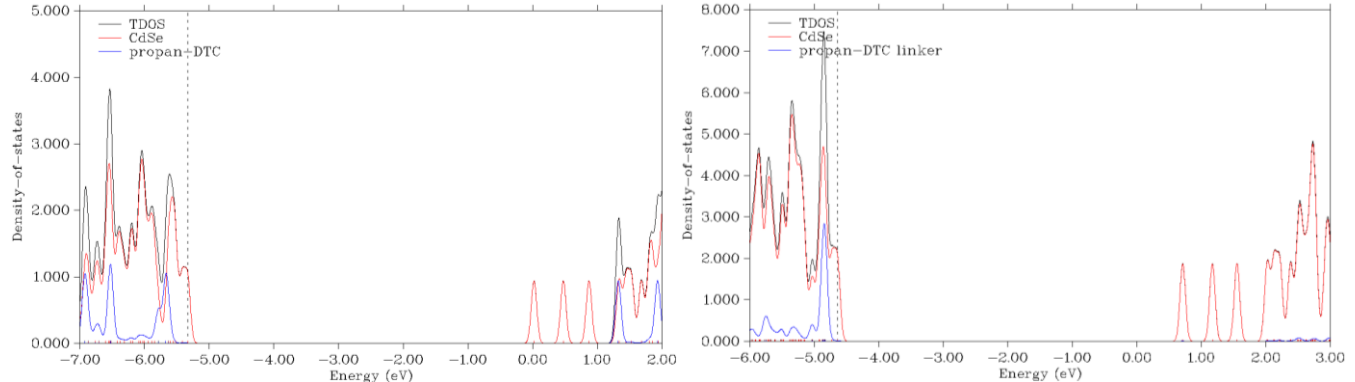


Figure S11: Projected density of states for monomer ($\text{Cd}_{13}\text{Se}_{13}$)-propan-DTC (left) and for dimer ($\text{Cd}_{13}\text{Se}_{13}$)-propanDTC -($\text{Cd}_{13}\text{Se}_{13}$) (right) obtained with Mulliken scheme (FWHM=0.1eV). NTT ligand states reported in blue and $\text{Cd}_{13}\text{Se}_{13}$ states in red. Black line represents the total density of states (TDOS). Vertical dashed lines point to HOMO orbitals

4.2. simulated spectra of monomer ($\text{Cd}_{13}\text{Se}_{13}$)-propanDTC and dimer of ($\text{Cd}_{13}\text{Se}_{13}$)-propanDTC-($\text{Cd}_{13}\text{Se}_{13}$)

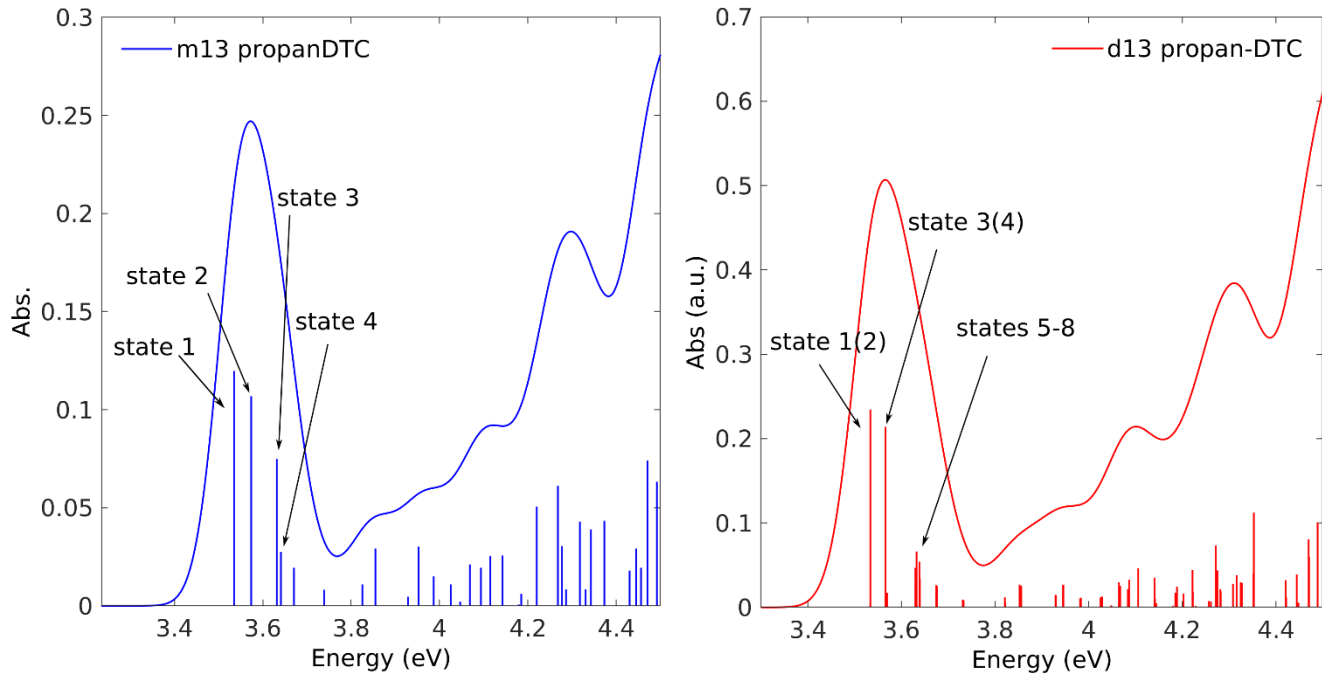
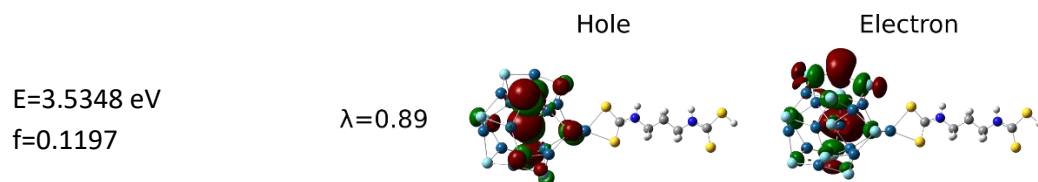


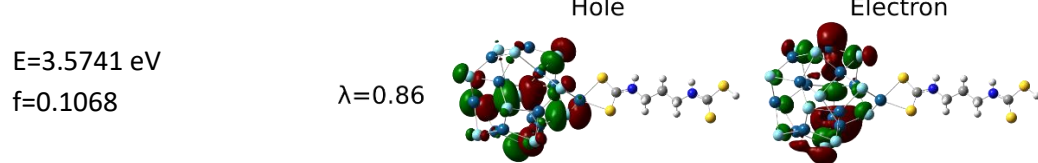
Figure S12: Simulated absorption spectra ($\sigma=0.05\text{eV}$) of monomer ($\text{Cd}_{13}\text{Se}_{13}$)-propanDTC (left, blue) and of dimer ($\text{Cd}_{13}\text{Se}_{13}$)-propanDTC-($\text{Cd}_{13}\text{Se}_{13}$) (right, red). First excited states are progressively numbered. Between parentheses, the excited states with low oscillator strength, difficult to pinpoint by eye, are reported.

4.3. Natural transition orbitals of monomer ($\text{Cd}_{13}\text{Se}_{13}$)-propan DTC

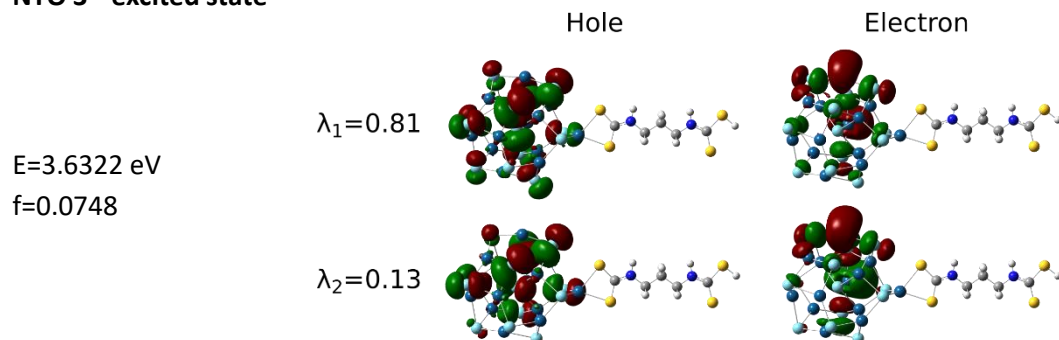
NTO 1st excited state



NTO 2nd excited state



NTO 3rd excited state



NTO 4th excited state

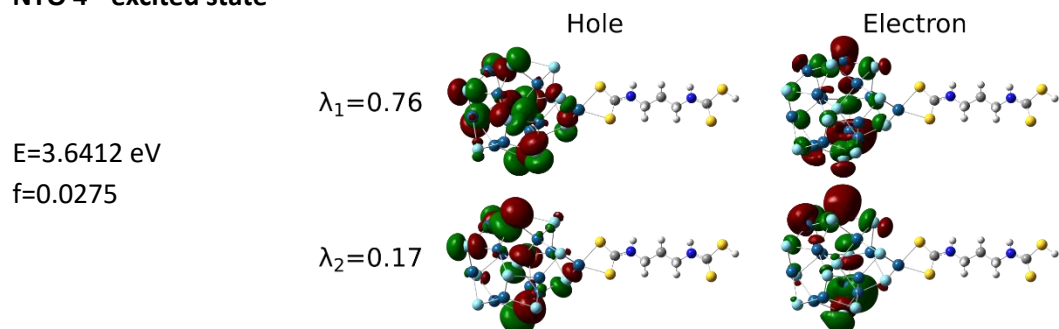
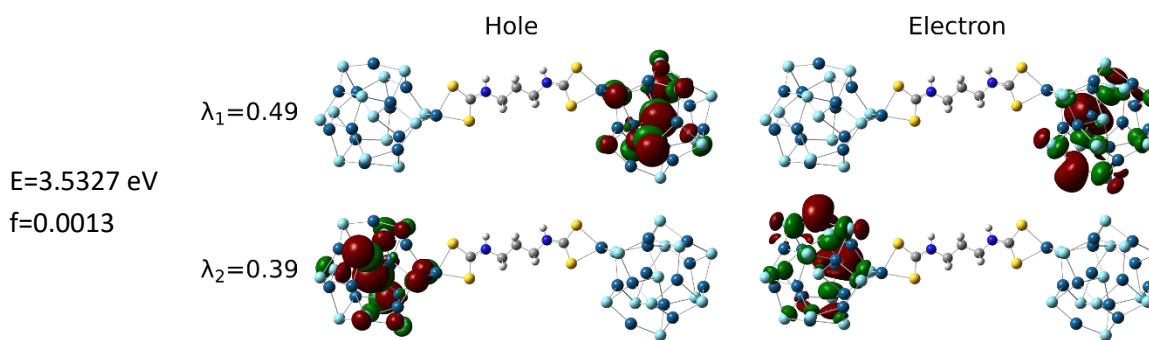


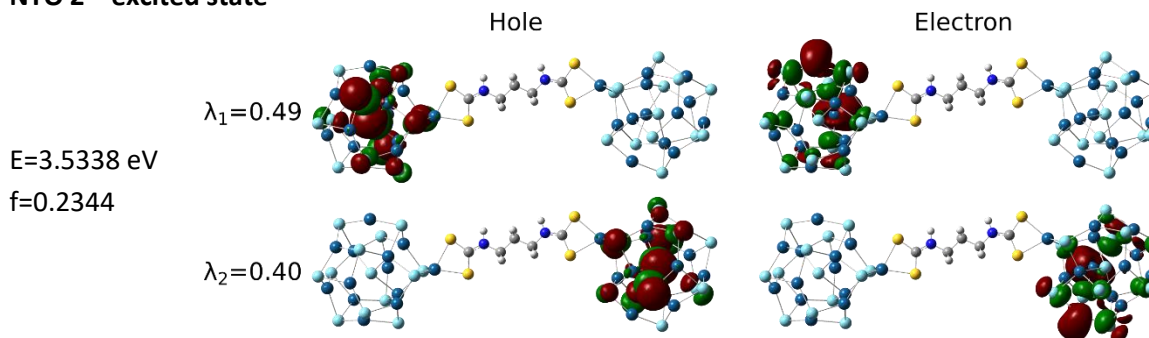
Figure S13: NTOs of representative low-energy excites states of monomer ($\text{Cd}_{13}\text{Se}_{13}$)-propanDTC

4.4. Natural transition orbitals of dimer ($\text{Cd}_{13}\text{Se}_{13}$)-propanDTC-($\text{Cd}_{13}\text{Se}_{13}$)

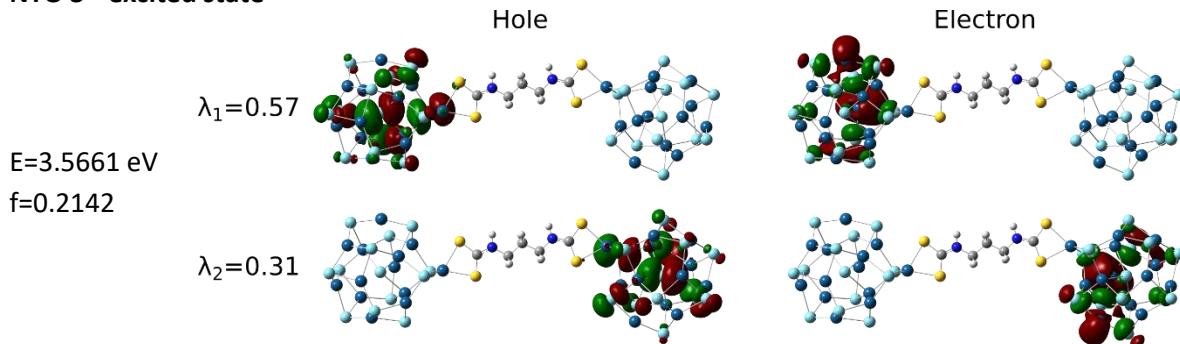
NTO 1st excited state



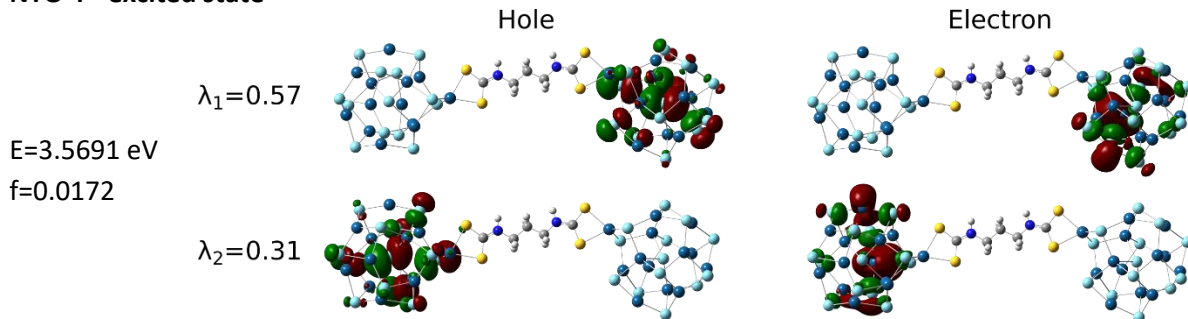
NTO 2nd excited state



NTO 3rd excited state



NTO 4th excited state



NTO 5th excited state

E=3.6293 eV

f=0.0468

Local excitation on a single dot

NTO 6th excited state

E=3.6156 eV

f=0.0094

Local excitation on a single dot

Figure S14: NTOs of representative low-energy excites states of dimer ($\text{Cd}_{13}\text{Se}_{13}$)-propanDTC-($\text{Cd}_{13}\text{Se}_{13}$)

5. Comparison between PDTC and propan-DTC

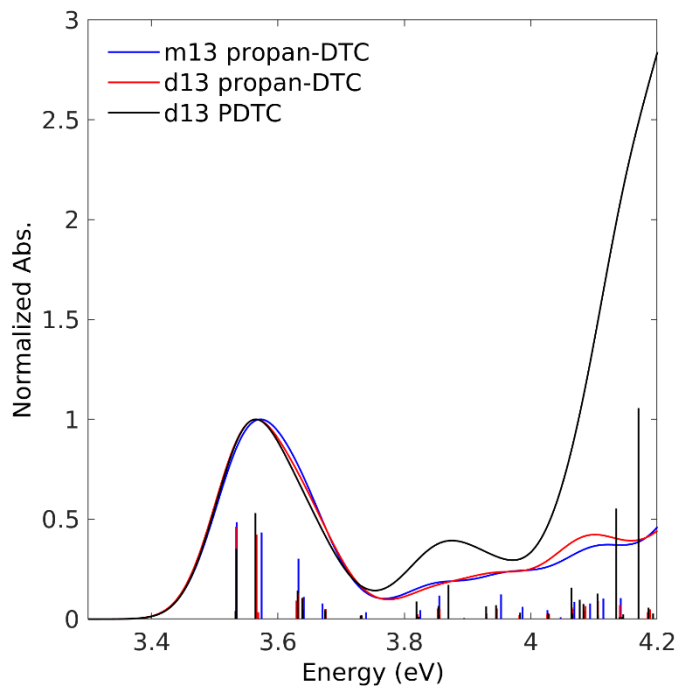


Figure S15: Normalized spectra of monomer ($\text{Cd}_{13}\text{Se}_{13}$)-propanDTC (blue), dimer ($\text{Cd}_{13}\text{Se}_{13}$)-propanDTC-($\text{Cd}_{13}\text{Se}_{13}$) (red), dimer ($\text{Cd}_{13}\text{Se}_{13}$)-PDTC-($\text{Cd}_{13}\text{Se}_{13}$) (black)

6. Details on the electronic structure of $(\text{Cd}_{13}\text{Se}_{13})\text{-BTT-(Cd}_{13}\text{Se}_{13})$

6.1. Density of states of monomer $(\text{Cd}_{13}\text{Se}_{13})\text{-BTT}$ and dimer of $(\text{Cd}_{13}\text{Se}_{13})\text{-BTT-(Cd}_{13}\text{Se}_{13})$

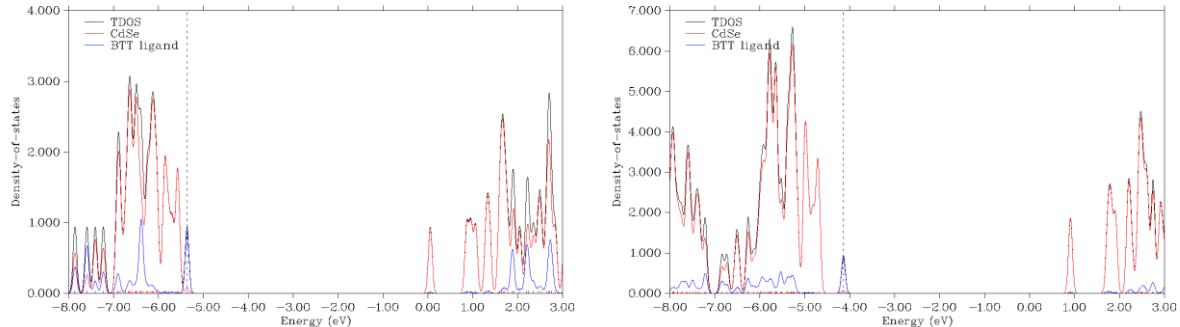


Figure S16: Projected density of states for monomer $(\text{Cd}_{13}\text{Se}_{13})\text{-BTT}$ (left) and for dimer $(\text{Cd}_{13}\text{Se}_{13})\text{-BTT-(Cd}_{13}\text{Se}_{13})$ (right) obtained with Mulliken scheme (FWHM=0.1eV). BTT ligand states reported in blue and $\text{Cd}_{13}\text{Se}_{13}$ states in red. Black line represents the total density of states (TDOS).

6.2. Simulated spectra of monomer $(\text{Cd}_{13}\text{Se}_{13})\text{-BTT}$ and dimer of $(\text{Cd}_{13}\text{Se}_{13})\text{-BTT-(Cd}_{13}\text{Se}_{13})$

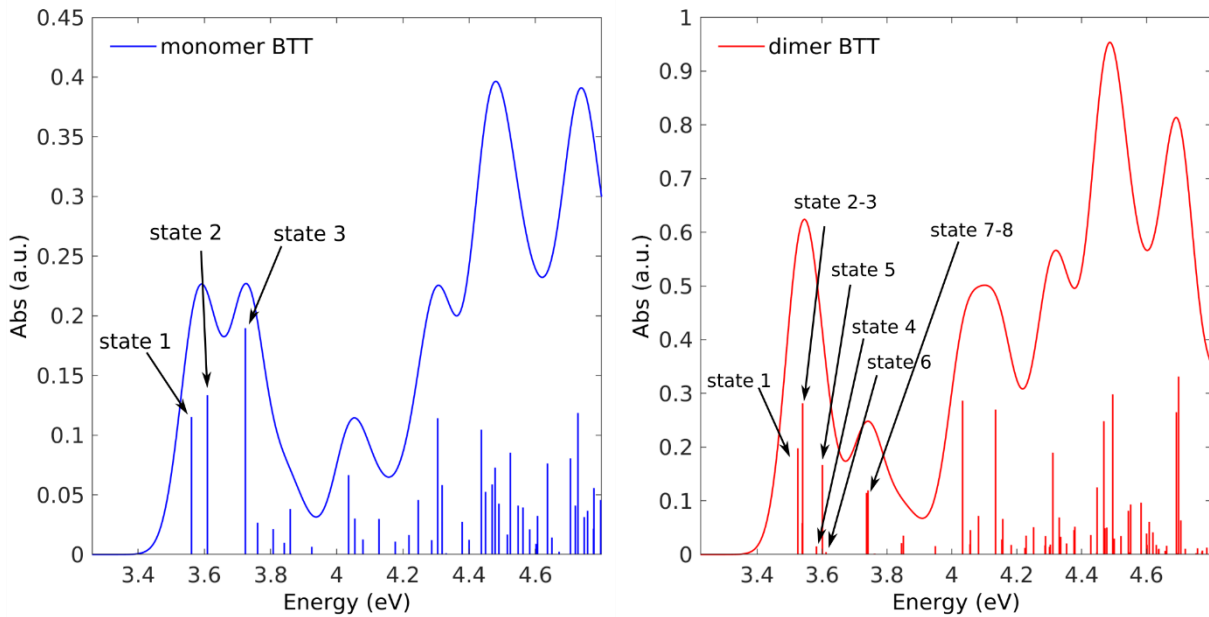
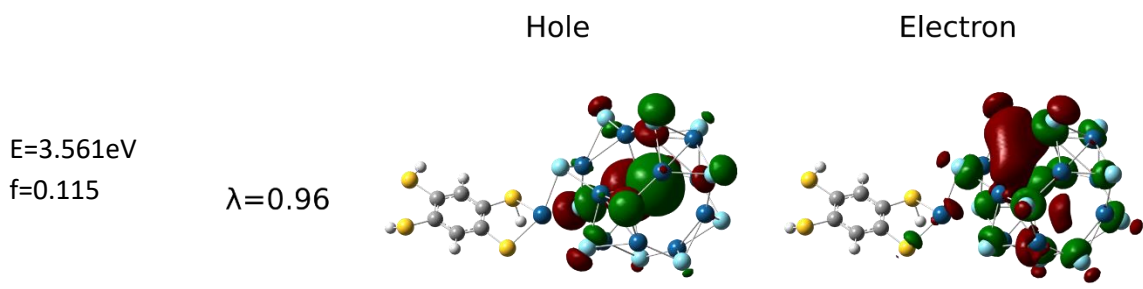


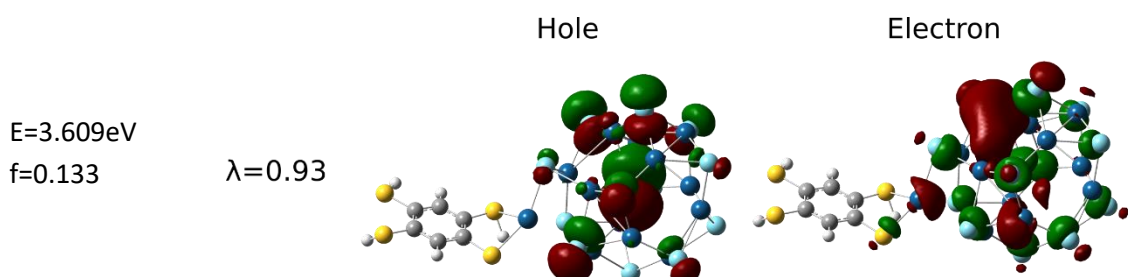
Figure S17: Simulated absorption spectra ($\sigma=0.05\text{eV}$) of monomer $(\text{Cd}_{13}\text{Se}_{13})\text{-BTT}$ (left, blue) and of dimer $(\text{Cd}_{13}\text{Se}_{13})\text{-BTT-(Cd}_{13}\text{Se}_{13})$ (right, red). First excited states are progressively numbered.

6.3. Natural transition orbitals monomer ($Cd_{13}Se_{13}$)-BTT

NTO 1st excited state



NTO 2nd excited state



NTO 3rd excited state

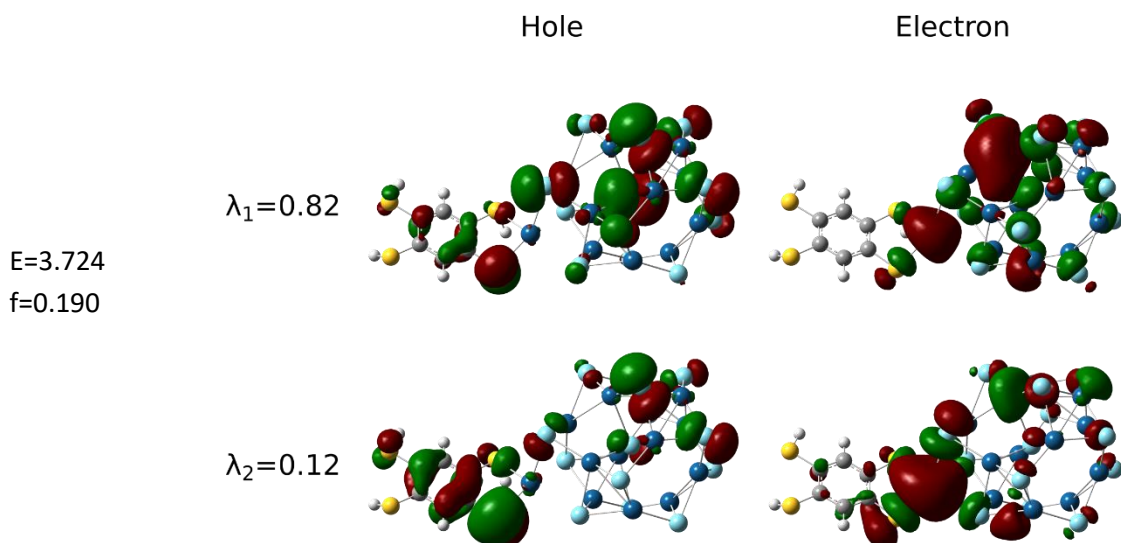
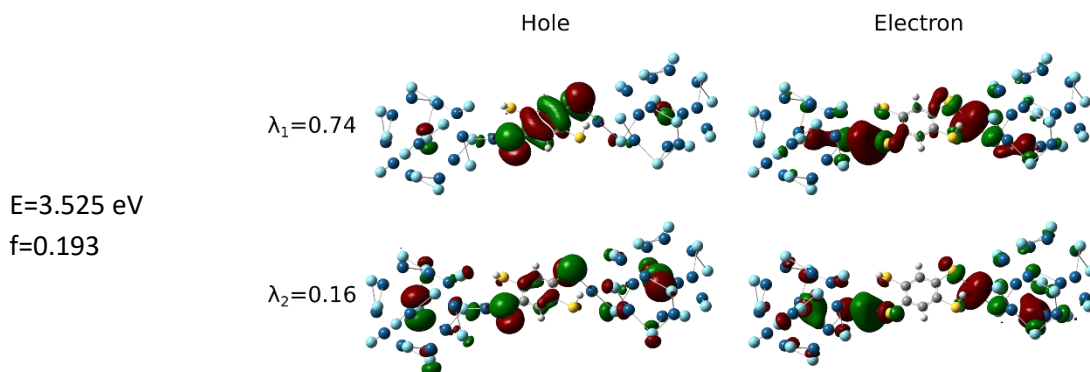


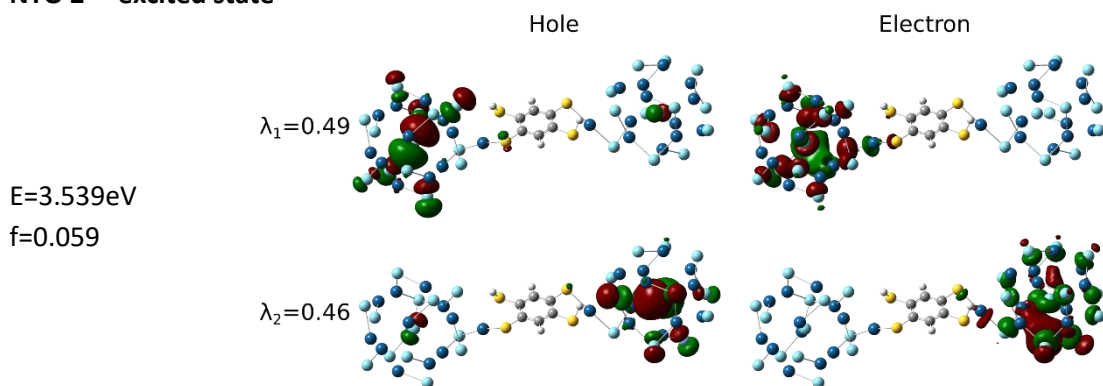
Figure S18: NTOs of representative low-energy excites states of monomer ($\text{Cd}_{13}\text{Se}_{13}$)-BTT.

6.4. Natural transition orbitals of dimer of $(Cd_{13}Se_{13})$ -BTT- $(Cd_{13}Se_{13})$

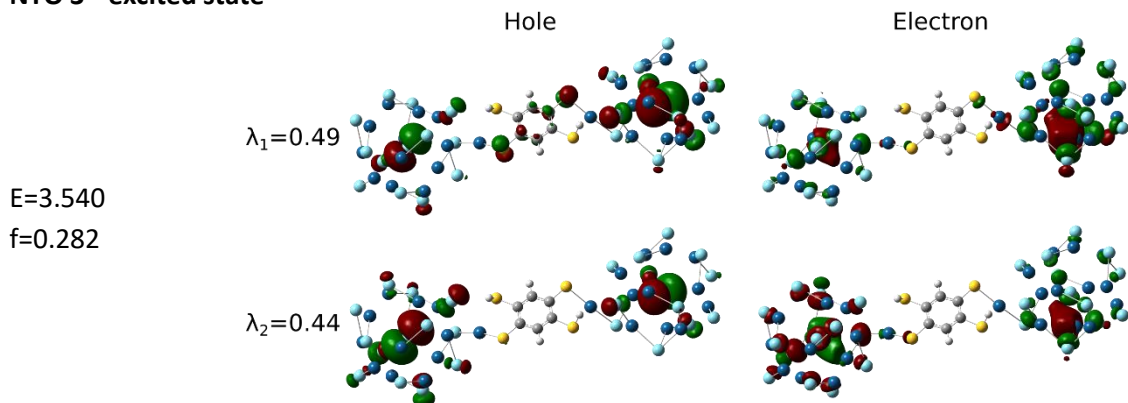
NTO 1st excited state



NTO 2nd excited state



NTO 3rd excited state



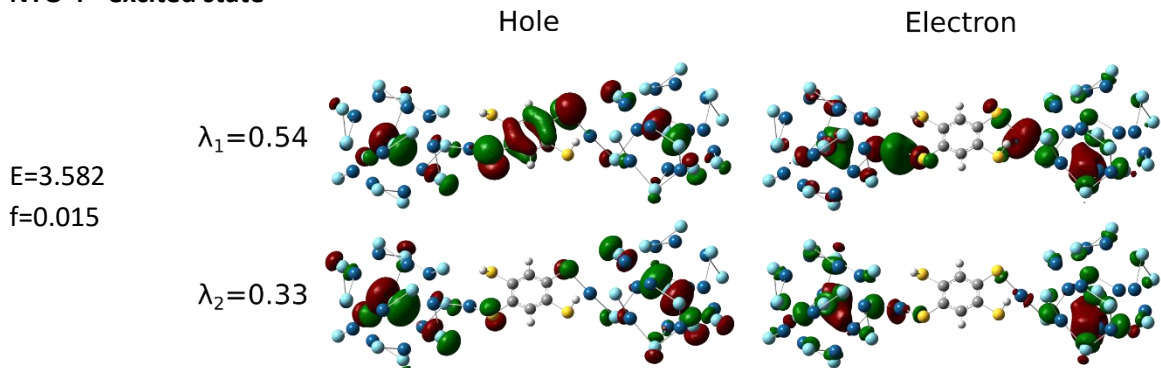
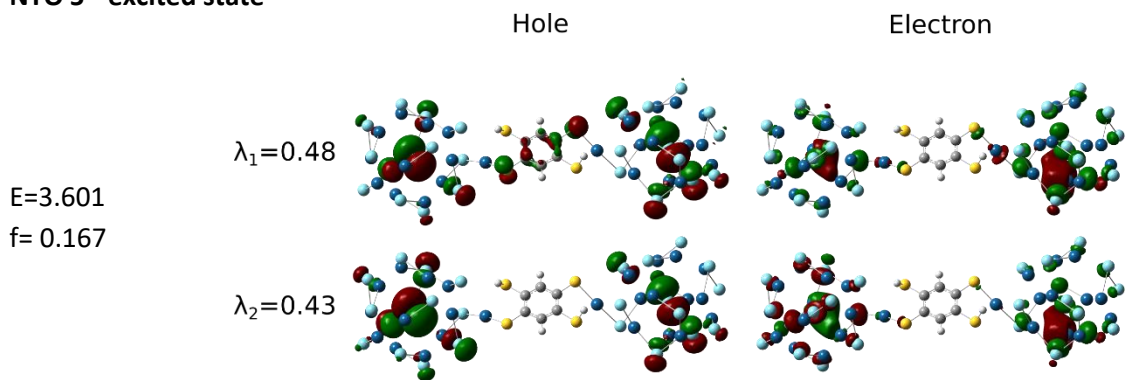
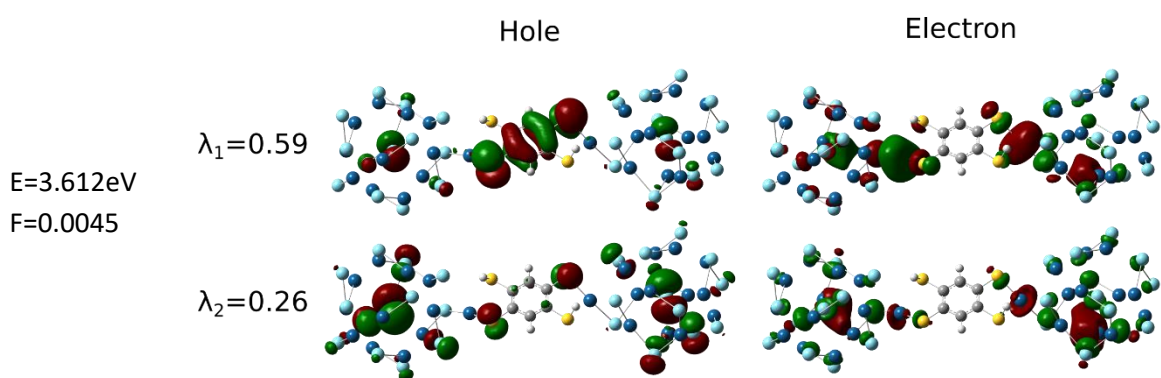
NTO 4th excited state**NTO 5th excited state****NTO 6th excited state**

Figure S19: NTOs of representative low-energy excites states of dimer ($\text{Cd}_{13}\text{Se}_{13}$)-BTT-($\text{Cd}_{13}\text{Se}_{13}$)

7. Details on the electronic structure of $(\text{Cd}_{13}\text{Se}_{13})\text{-NTT-(Cd}_{13}\text{Se}_{13})$

7.1. Density of states of monomer $(\text{Cd}_{13}\text{Se}_{13})\text{-NTT}$ and dimer of $(\text{Cd}_{13}\text{Se}_{13})\text{-NTT-(Cd}_{13}\text{Se}_{13})$

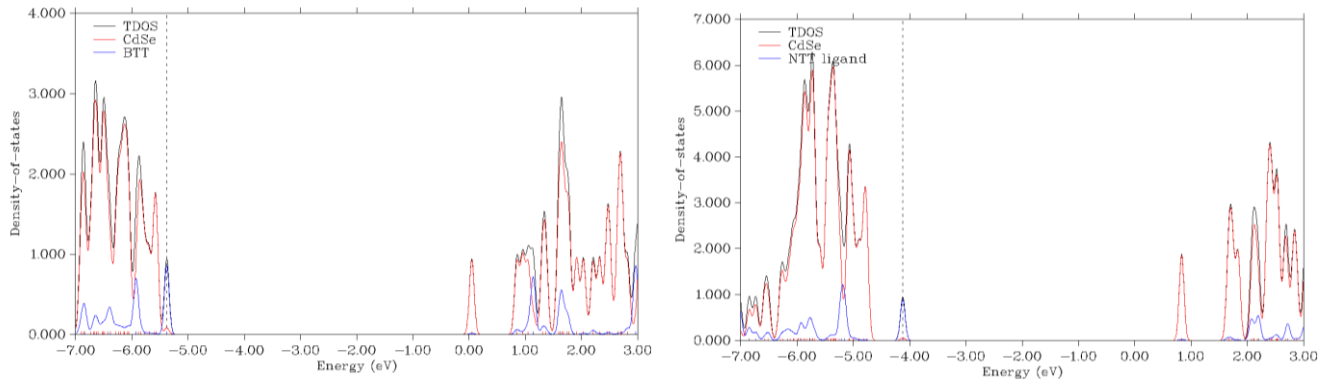


Figure S20: Projected density of states for monomer $(\text{Cd}_{13}\text{Se}_{13})\text{-NTT}$ (left) and for dimer $(\text{Cd}_{13}\text{Se}_{13})\text{-NTT-(Cd}_{13}\text{Se}_{13})$ (right) obtained with Mulliken scheme (FWHM=0.1eV). NTT ligand states reported in blue and $\text{Cd}_{13}\text{Se}_{13}$ states in red. Black line represents the total density of states (TDOS). Vertical dashed lines point to HOMO orbitals

7.2. Simulated spectra of monomer $(\text{Cd}_{13}\text{Se}_{13})\text{-NTT}$ and dimer of $(\text{Cd}_{13}\text{Se}_{13})\text{-NTT-(Cd}_{13}\text{Se}_{13})$

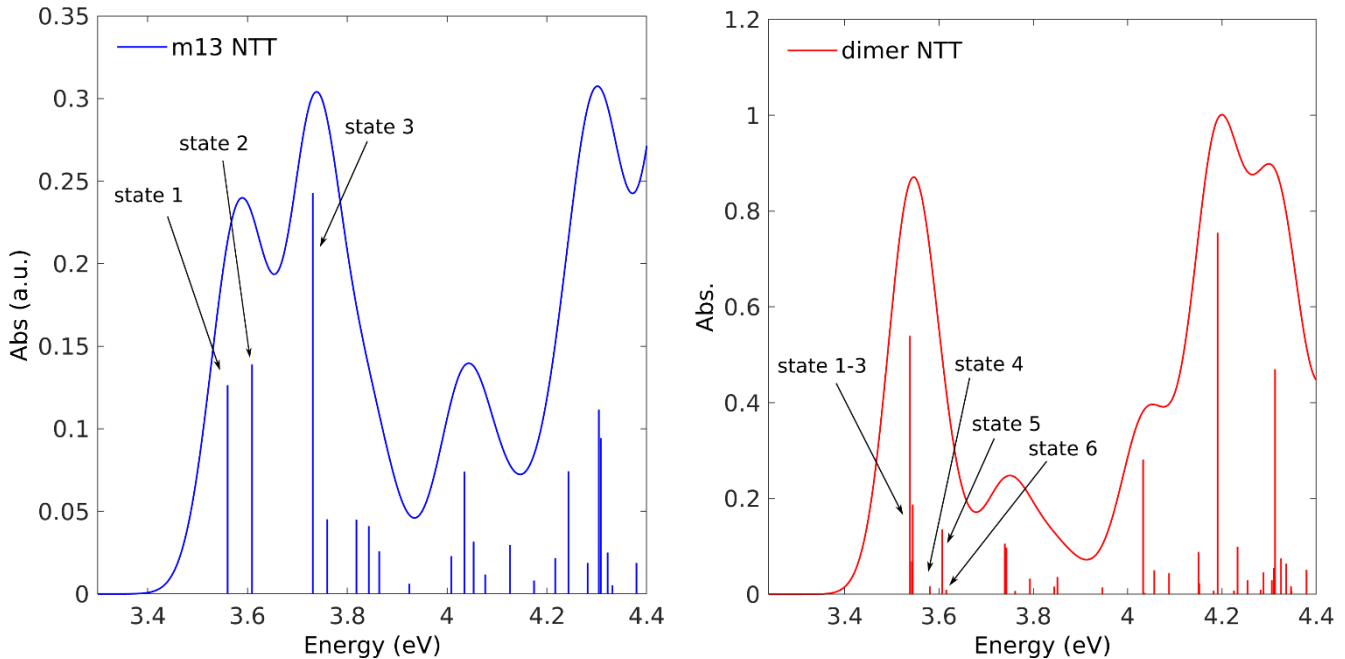


Figure S21: Simulated absorption spectra ($\sigma=0.05\text{eV}$) of monomer $(\text{Cd}_{13}\text{Se}_{13})\text{-NTT}$ (left, blue) and of dimer $(\text{Cd}_{13}\text{Se}_{13})\text{-NTT-(Cd}_{13}\text{Se}_{13})$ (right, red). First excited states are progressively numbered.

7.3. Frontier Orbitals of monomer ($\text{Cd}_{13}\text{Se}_{13}$)-NTT

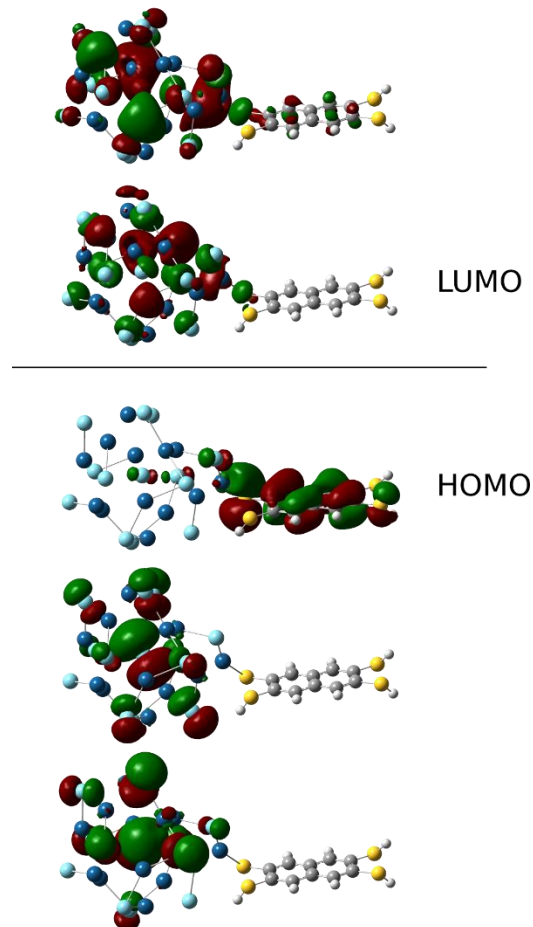
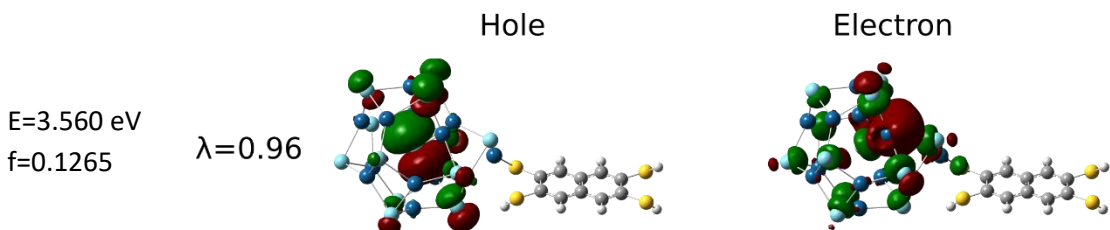


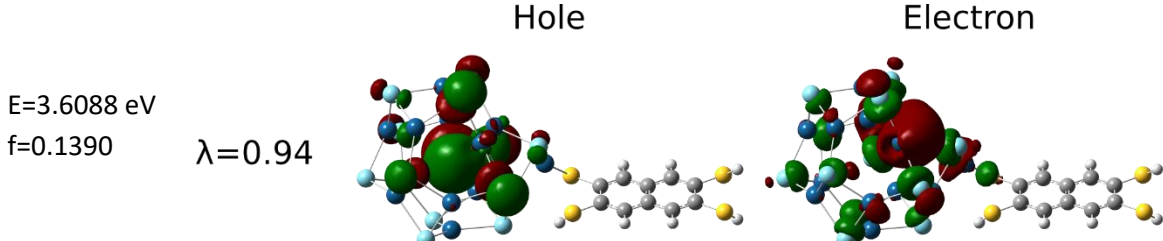
Figure S22: Monomer ($\text{Cd}_{13}\text{Se}_{13}$)-NTT representative frontiers orbitals reported as level scheme

7.4. Natural transition orbitals of monomer ($\text{Cd}_{13}\text{Se}_{13}$)-NTT

NTO 1st excited state



NTO 2nd excited state



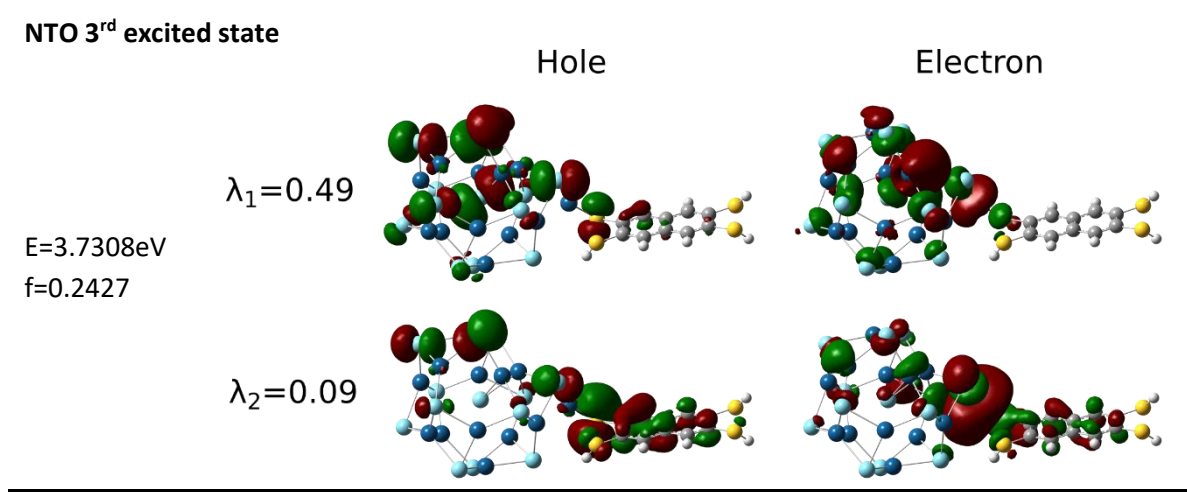


Figure S23: NTOs of representative low-energy excites states of monomer ($\text{Cd}_{13}\text{Se}_{13}$)-NTT

7.5. Frontier orbitals of dimer ($\text{Cd}_{13}\text{Se}_{13}$)-NTT-($\text{Cd}_{13}\text{Se}_{13}$)

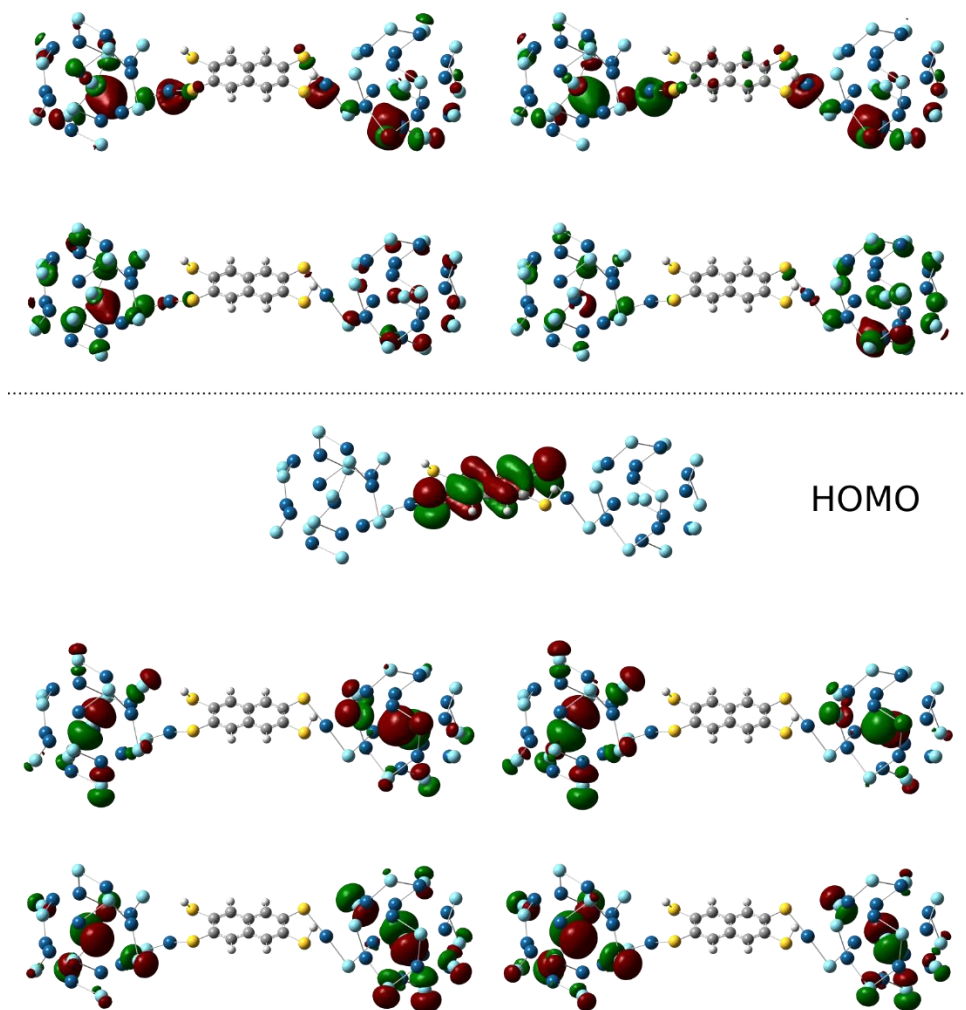
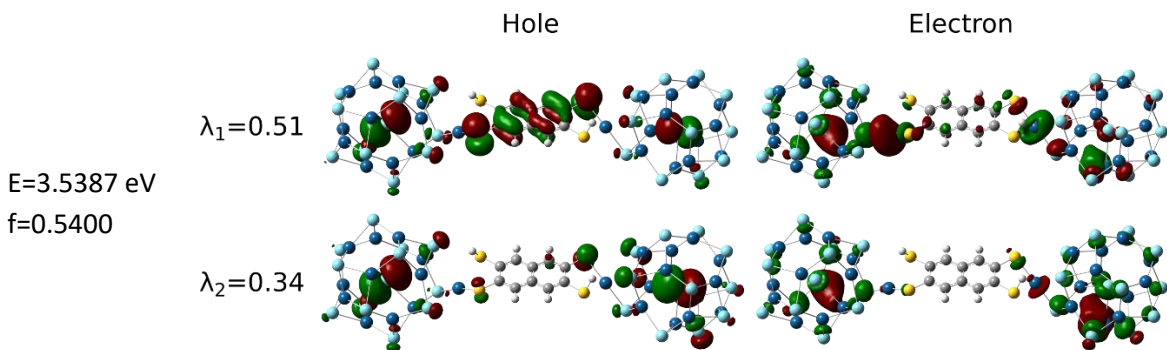


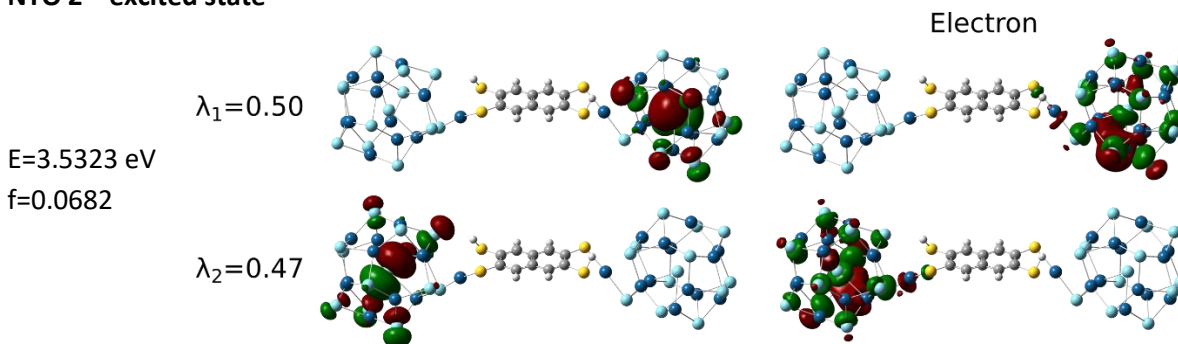
Figure S24: Dimer ($\text{Cd}_{13}\text{Se}_{13}$)-NTT-($\text{Cd}_{13}\text{Se}_{13}$) representative frontiers orbitals reported as level scheme.

7.6. Natural transition orbitals of dimer ($\text{Cd}_{13}\text{Se}_{13}$)-NTT-($\text{Cd}_{13}\text{Se}_{13}$)

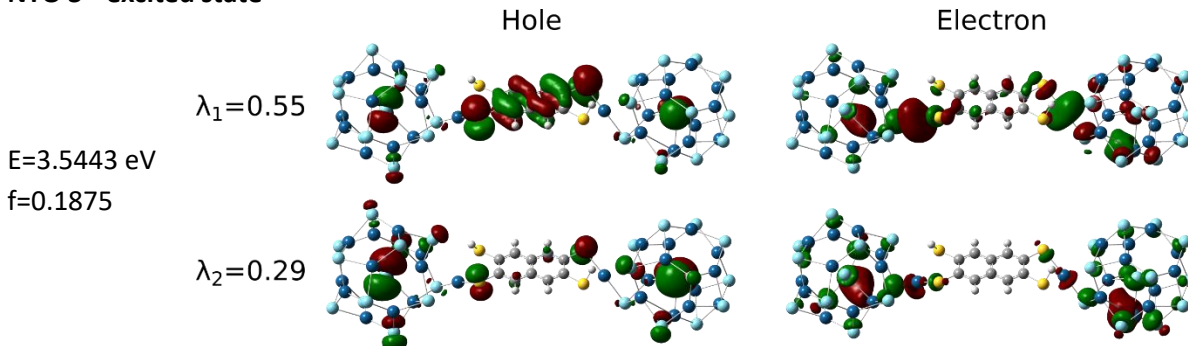
NTO 1st excited state



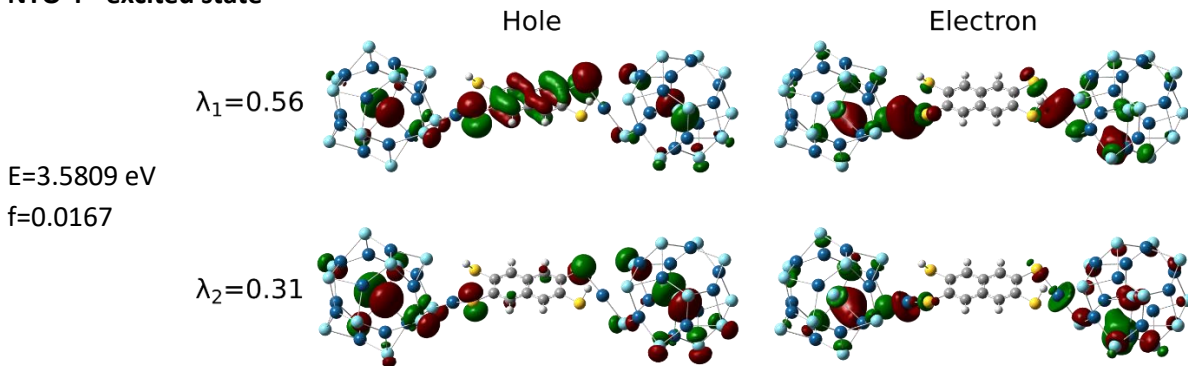
NTO 2nd excited state



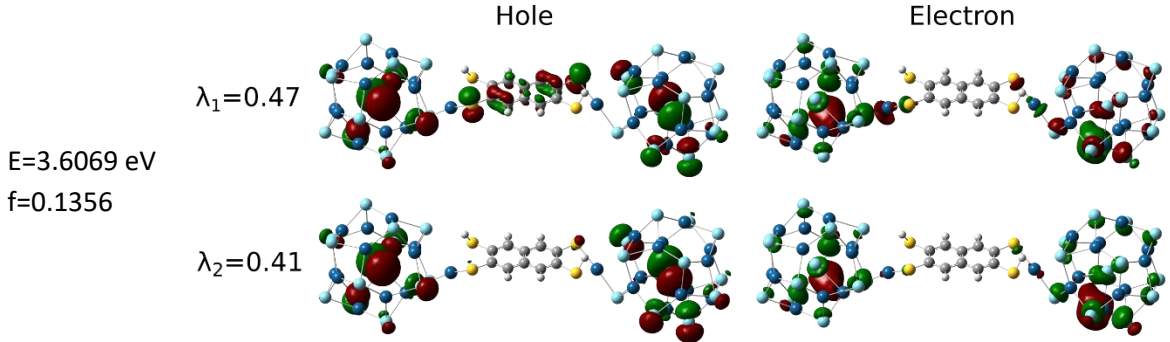
NTO 3rd excited state



NTO 4th excited state



NTO 5th excited state



NTO 6th excited state

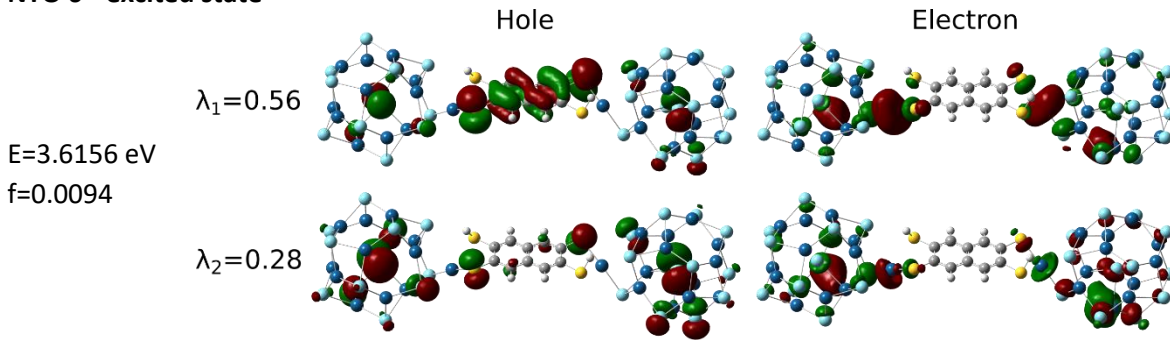


Figure S25: NTOs of representative low-energy excites states of dimer ($\text{Cd}_{13}\text{Se}_{13}$)-NTT-($\text{Cd}_{13}\text{Se}_{13}$)

8. Comparison between BTT and NTT

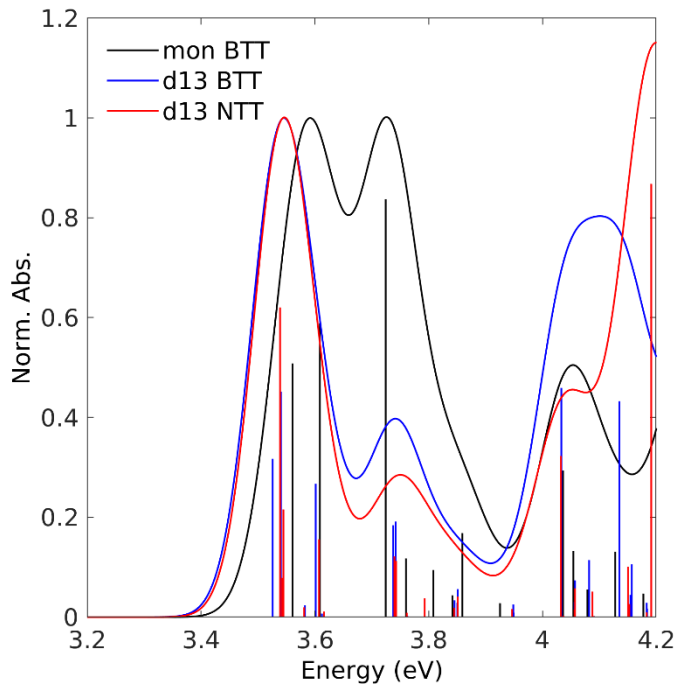


Figure S26: Normalized spectra of monomer ($\text{Cd}_{13}\text{Se}_{13}$)-BTT (black), dimer ($\text{Cd}_{13}\text{Se}_{13}$)-BTT-($\text{Cd}_{13}\text{Se}_{13}$) (blue), dimer ($\text{Cd}_{13}\text{Se}_{13}$)-NTT-($\text{Cd}_{13}\text{Se}_{13}$) (red)

9. Details on the electronic structure of $\text{Cd}_{17}\text{Se}_4(\text{SCH}_3)_{26}$ -Py-Py- $\text{Cd}_{17}\text{Se}_4(\text{SCH}_3)_{26}$

9.1. Density of states of monomer $\text{Cd}_{17}\text{Se}_4(\text{SCH}_3)_{26}$ -Py and dimer $\text{Cd}_{17}\text{Se}_4(\text{SCH}_3)_{26}$ -Py-Py- $\text{Cd}_{17}\text{Se}_4(\text{SCH}_3)_{26}$

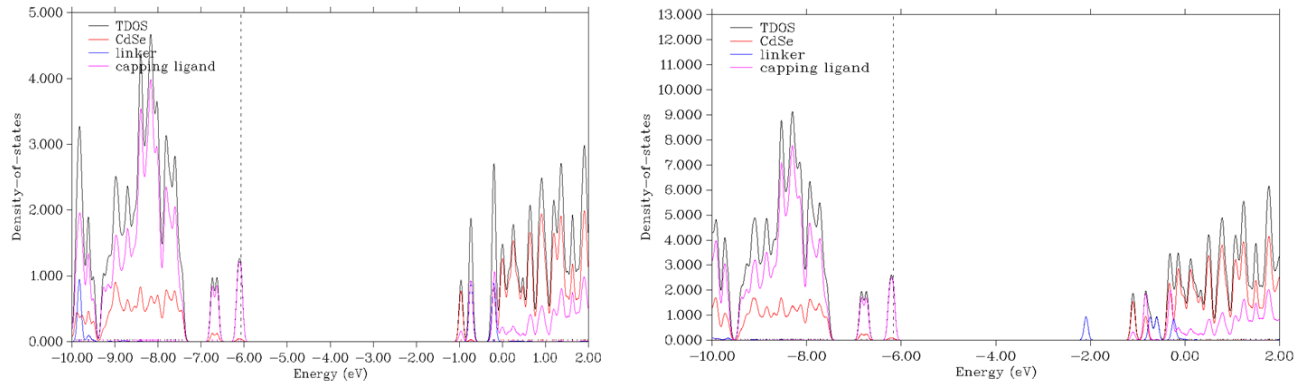


Figure S27: Projected density of states for monomer $\text{Cd}_{17}\text{Se}_4(\text{SCH}_3)_{26}$ -Py (left) and for dimer $\text{Cd}_{17}\text{Se}_4(\text{SCH}_3)_{26}$ -Py-Py- $\text{Cd}_{17}\text{Se}_4(\text{SCH}_3)_{26}$ (right), obtained with Mulliken scheme (FWHM=0.1eV). PDTc ligand states reported in blue and $\text{Cd}_{13}\text{Se}_{13}$ states in red. Black line represents the total density of states (TDOS).

9.2. Simulated spectra of monomer $\text{Cd}_{17}\text{Se}_4(\text{SCH}_3)_{26}$ -Py

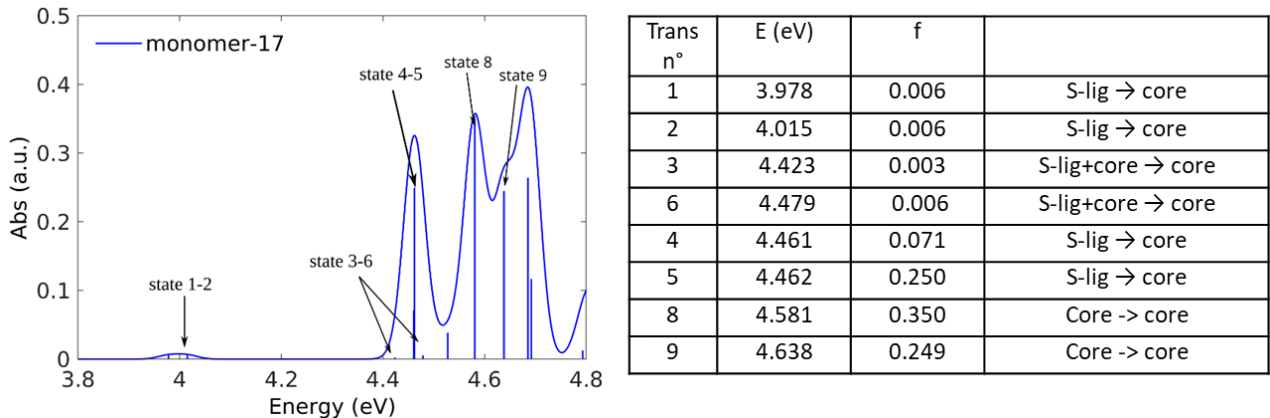
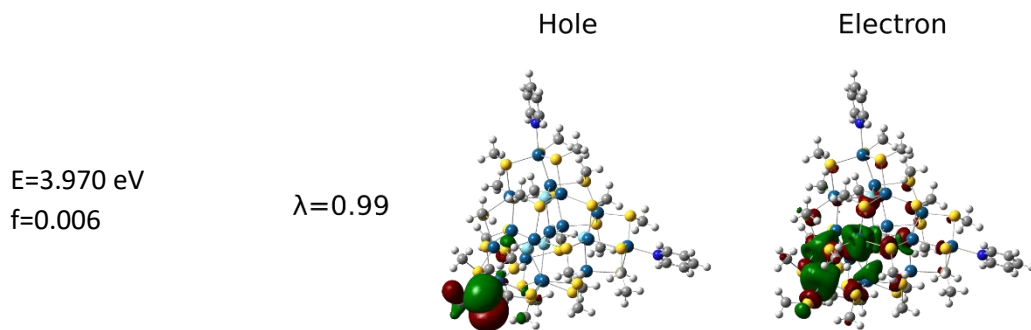


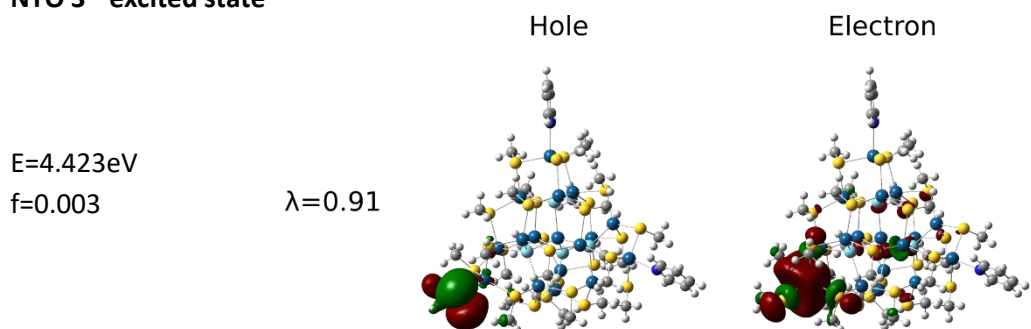
Figure S28: Simulated absorption spectra ($\sigma=0.04\text{eV}$) of monomer $\text{Cd}_{17}\text{Se}_4(\text{SCH}_3)_{26}$ -Py is reported in blue on the left where the firsts excited states are progressively numbered. Table on the right reports energy (E), oscillator strength (f) and description of the selected low energy excited states.

9.3. Natural transition orbitals of monomer Cd₁₇Se₄(SCH₃)₂₆-Py

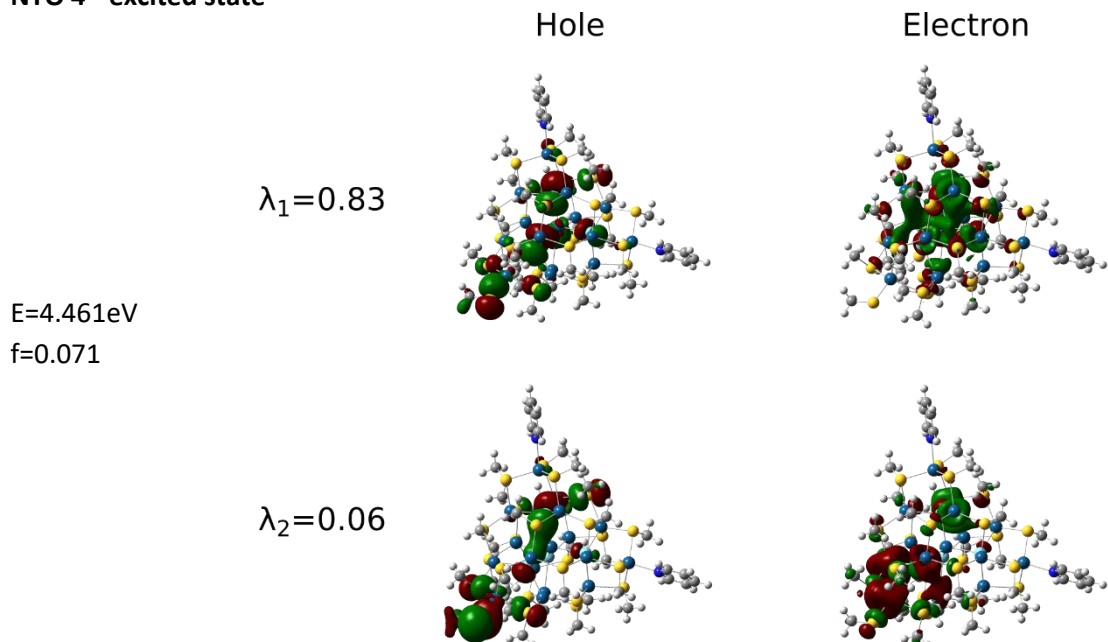
NTO 1st excited state



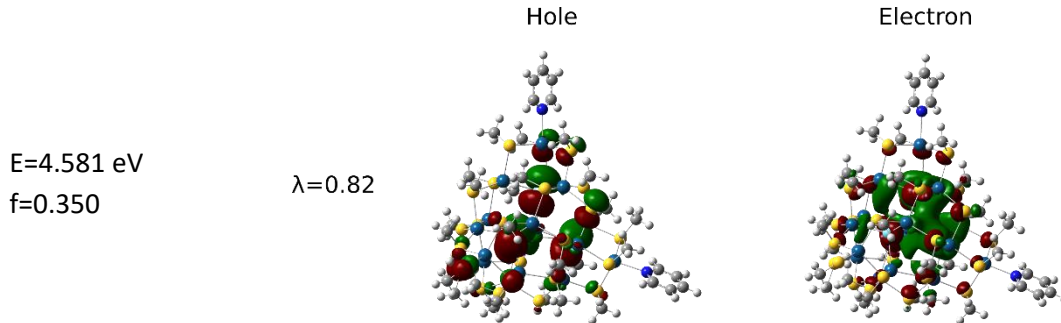
NTO 3rd excited state



NTO 4th excited state



NTO 8th excited state



NTO 9th excited state

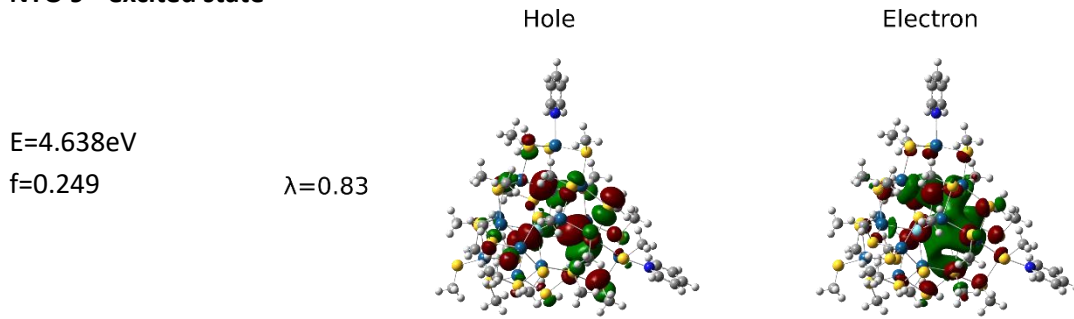


Figure S29: NTOs of representative low-energy excites states of monomer $\text{Cd}_{17}\text{Se}_4(\text{SCH}_3)_{26}\text{-Py}$

9.4. Simulated spectra of dimer $\text{Cd}_{17}\text{Se}_4(\text{SCH}_3)_{26}\text{-Py-Py-Cd}_{17}\text{Se}_4(\text{SCH}_3)_{26}$

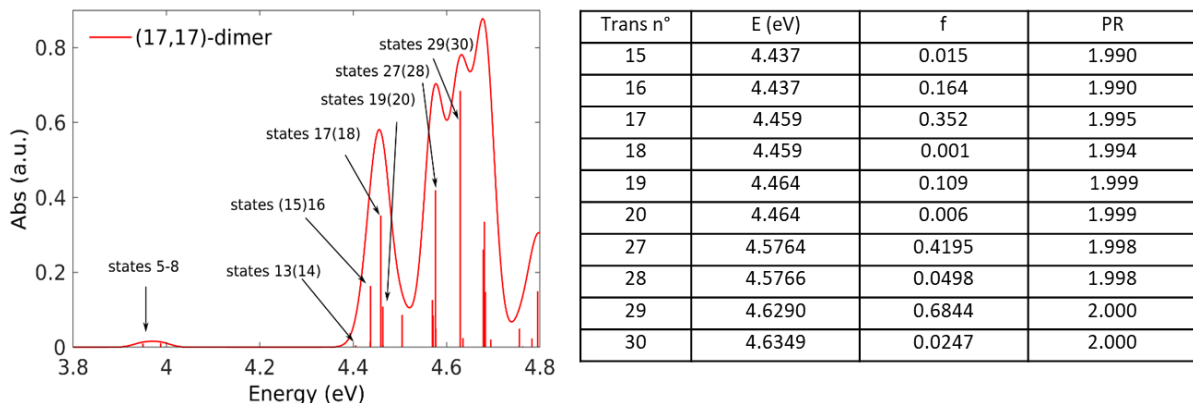
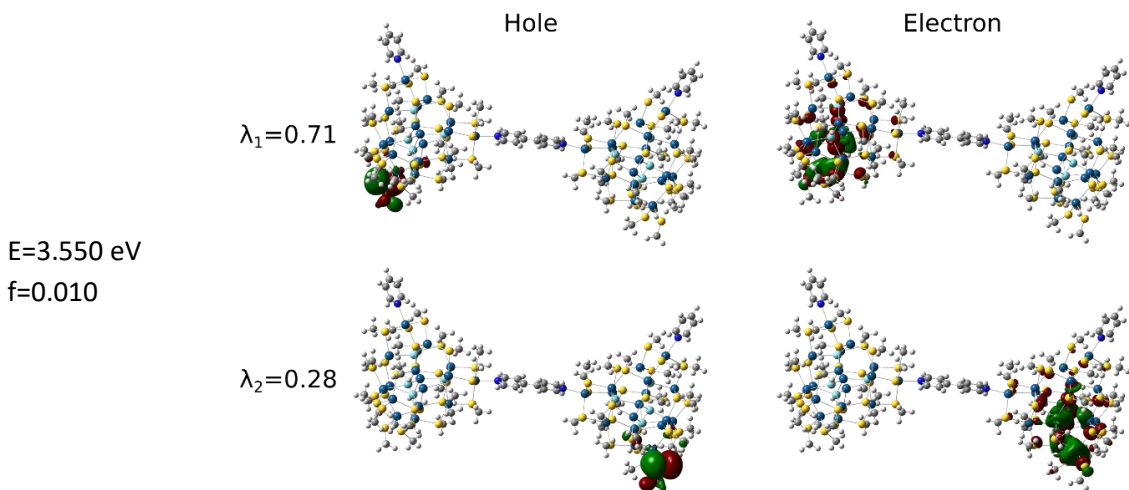


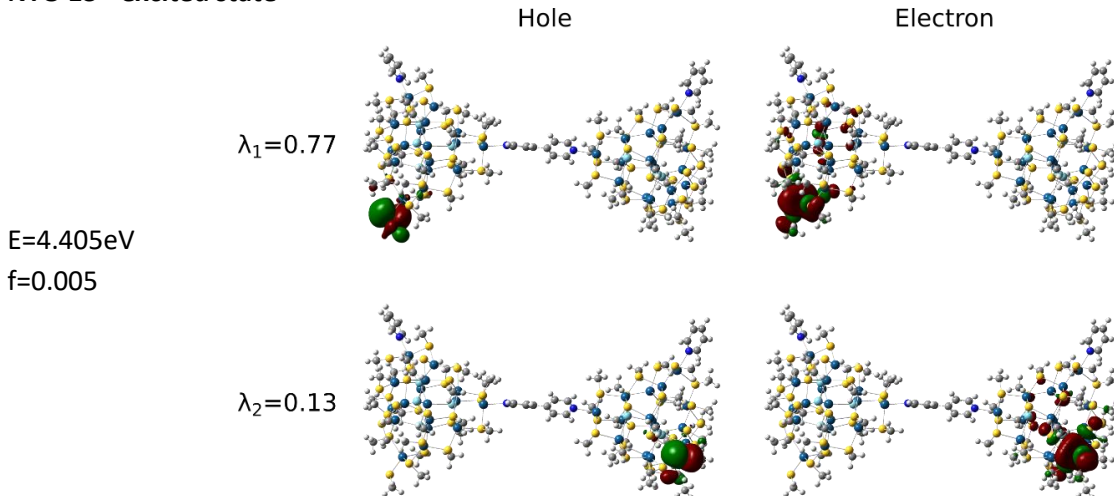
Figure S30: Simulated absorption spectra ($\sigma=0.04\text{eV}$) of dimer $\text{Cd}_{17}\text{Se}_4(\text{SCH}_3)_{26}\text{-Py- Cd}_{17}\text{Se}_4(\text{SCH}_3)_{26}$ is reported in red on the left where the firsts excited states are progressively numbered. Between parenthesis are reported the excited states with low oscillator strength and difficult to pinpoint by eye. Table on the right reports energy (E), oscillator strength (f) and description of selected low energy excited states.

9.5. Natural transition orbitals of dimer Cd₁₇Se₄(SCH₃)₂₆-Py-Py-Cd₁₇Se₄(SCH₃)₂₆

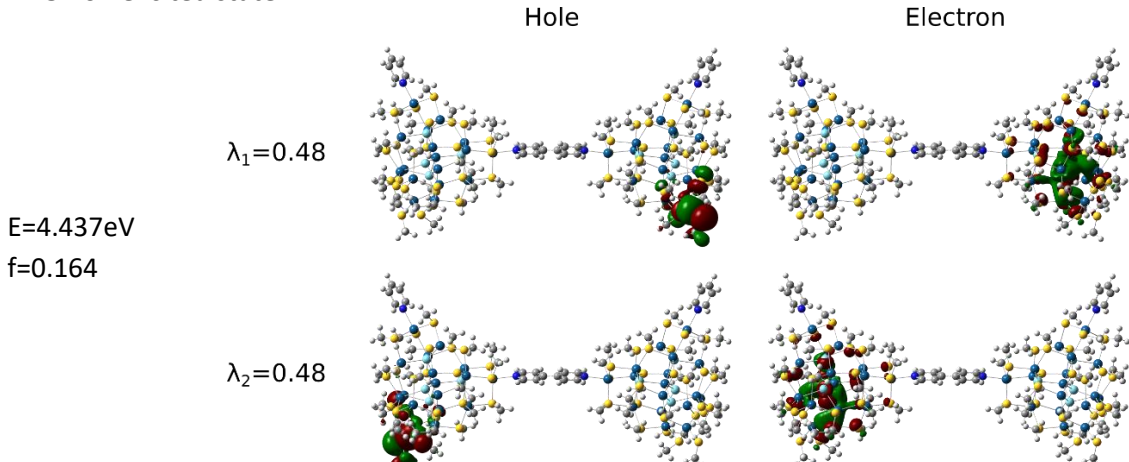
NTO 5th excited state



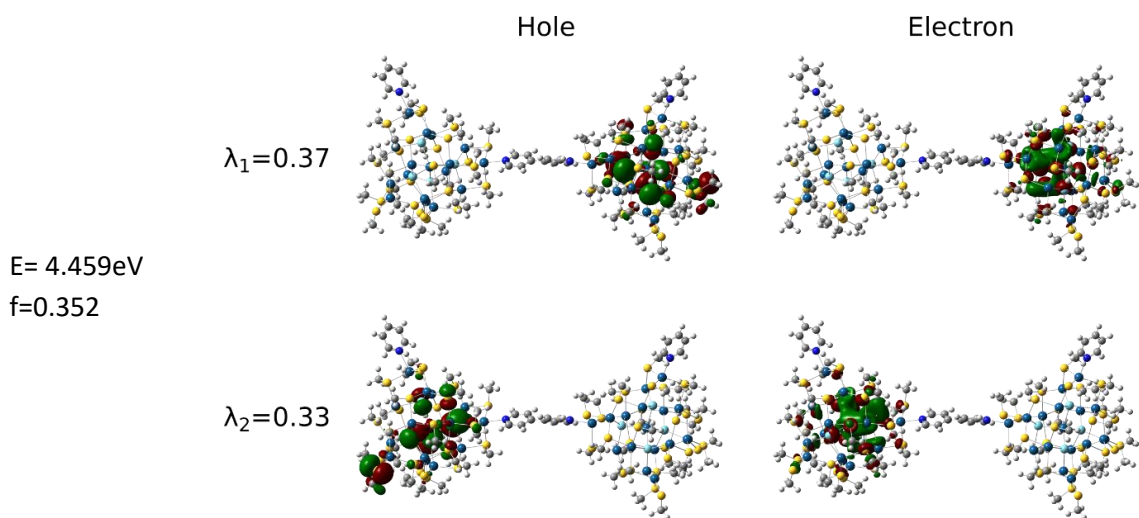
NTO 13th excited state



NTO 16th excited state



NTO 17th excited state



NTO 27th excited state

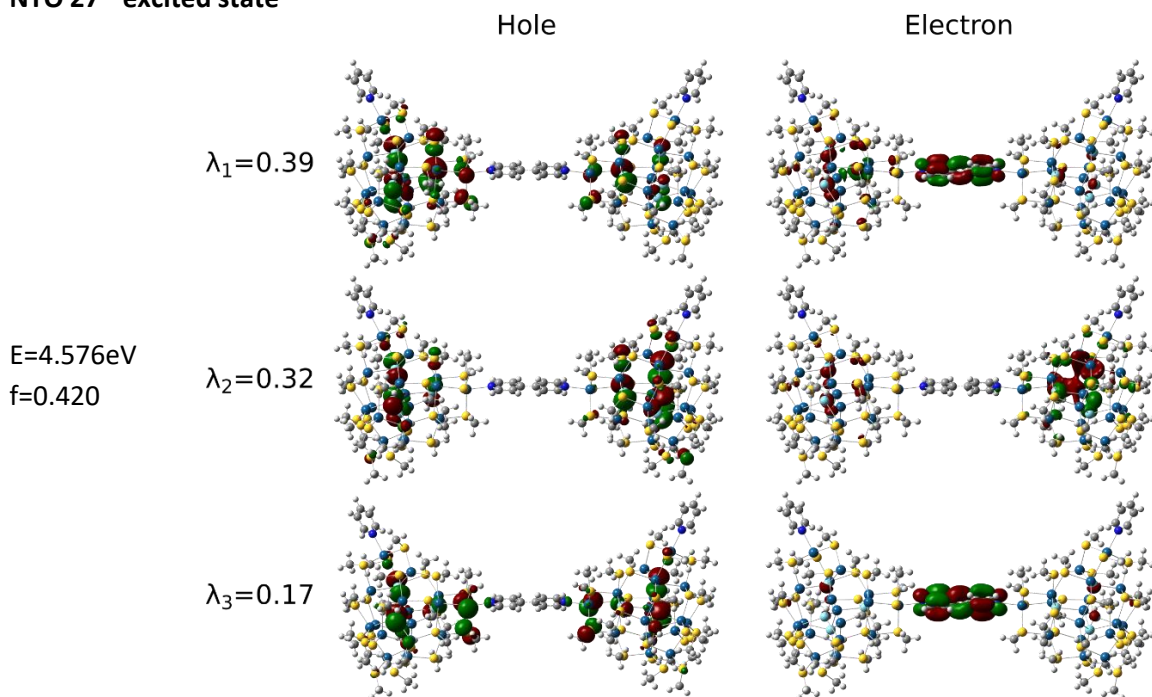
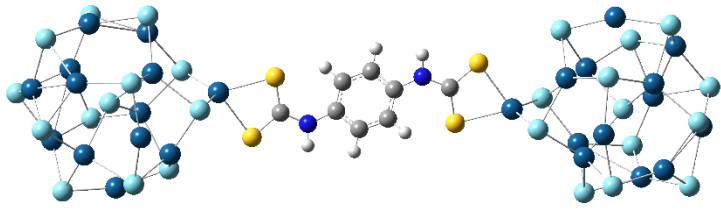
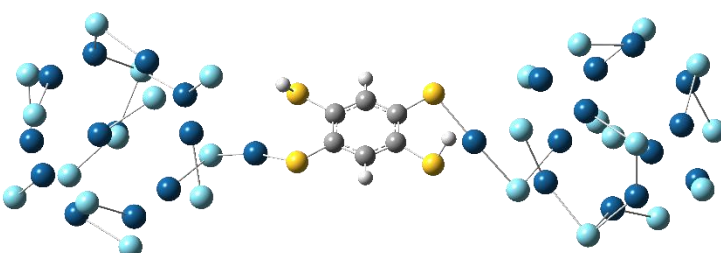
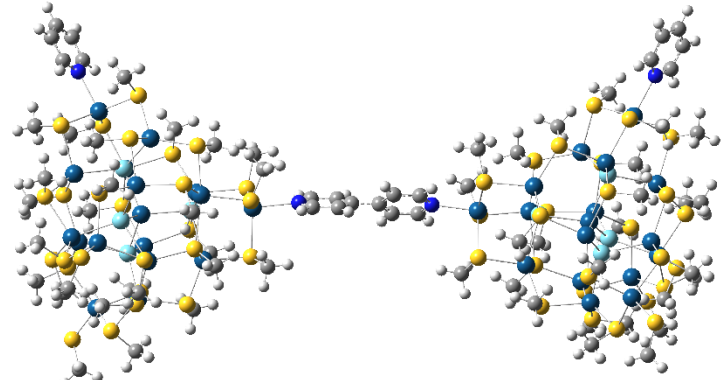
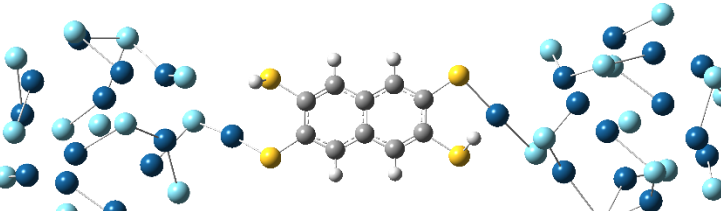


Figure S31: NTOs of representative low-energy excited states of dimer $\text{Cd}_{17}\text{Se}_4(\text{SCH}_3)_{26}\text{-Py-Py-Cd}_{17}\text{Se}_4(\text{SCH}_3)_{26}$

10. Structures, distances and coupling

Structure	D(QD-QD)	Red shift	Coupling
	1.34 nm	12 meV	Weak (2.25 meV)
	0.87 nm	47 meV	strong
	1.20 nm	6 meV	Very Weak
	1.11 nm	42 meV	strong

	1.33	6	Weak (splitting 0.55 meV)
--	------	---	---------------------------------

Table S2: structure of the QD dimers and relative distance between nearest QD atoms; red shift between monomer and dimer on first absorption peak of the simulated spectra; electronic coupling as semi-difference of first coupled excitons. For BTT and NTT systems the electronic coupling cannot be computed.

11.Optimized Coordinates

11.1. Cd₁₃Se₁₃-PDTC-Cd₁₃Se₁₃

Se	2.990469	2.936064	2.804616	H	-7.332547	-0.422749	-5.103273
Se	5.165481	-0.541825	0.152427	N	-6.573589	-0.612304	-5.748663
Se	3.044265	3.354072	-2.059333	C	-5.342052	-0.454681	-5.194258
Cd	3.549607	0.410204	2.185613	S	-3.897467	-0.546276	-6.139425
Cd	1.837736	3.451143	0.293001	S	-5.334936	-0.119286	-3.492871
Cd	3.773808	0.703917	-1.742117	N	-8.396326	-1.692724	-10.976999
Cd	0.352158	2.443852	3.114024	H	-7.636783	-1.888416	-11.619856
Cd	1.050670	1.973801	-3.391948	C	-9.626915	-1.839041	-11.536668
Cd	3.310995	-2.515997	0.529656	S	-11.075614	-1.729780	-10.599757
Se	-0.760557	3.955414	1.139990	S	-9.629474	-2.167928	-13.239358
Se	2.439171	-0.316751	-3.915794	Se	-18.307155	-0.412533	-15.667482
Se	2.660904	-2.031430	3.147817	Se	-18.118042	-2.570483	-20.041374
Se	-1.072778	0.514069	4.383286	Se	-19.950760	-5.051717	-16.254567
Se	2.036620	-4.081850	-1.244927	Cd	-17.072686	-1.053655	-17.917728
Se	-1.569089	2.353195	-3.316242	Cd	-18.738206	-3.057384	-14.977692
Cd	0.131029	-1.312420	2.542945	Cd	-18.410287	-4.740505	-18.530690
Cd	0.780717	-1.625052	-2.252982	Cd	-16.201781	-0.986020	-13.966230
Cd	-1.502733	2.001332	-0.628228	Cd	-17.885265	-6.813435	-15.925507
Se	0.558744	0.081823	0.084436	Cd	-15.437314	-2.854686	-20.210917
Se	-1.893385	-3.156494	1.850931	Se	-17.342587	-3.062418	-12.611389
Se	-3.964914	0.756786	0.198246	Se	-17.242718	-7.252838	-18.553749
Se	-1.783638	-2.451159	-2.657004	Se	-14.528945	-0.617417	-18.949250
Cd	-2.865623	0.845220	2.531540	Se	-13.638023	-0.379942	-14.232073
Cd	-0.145730	-4.107086	0.157822	Se	-13.784417	-4.946767	-20.716758
Cd	-2.662258	-0.085484	-3.820696	Se	-16.482373	-7.475238	-13.730276
Cd	-2.648090	-1.563762	-0.296880	Cd	-13.613980	-1.693366	-16.603308
C	-6.321194	-1.792063	-7.914536	Cd	-14.817851	-6.093254	-18.311038
C	-6.983493	-0.884433	-7.078527	Cd	-15.519371	-4.700168	-13.716289
C	-8.149372	-0.256684	-7.538772	Se	-15.440673	-3.952888	-16.521117
C	-8.649470	-0.511505	-8.811339	Se	-11.016354	-2.881143	-16.973274
C	-7.987331	-1.419123	-9.647435	Se	-12.887482	-5.038413	-13.097746
C	-6.821196	-2.046815	-9.187001	Se	-12.619926	-7.328916	-17.037864
H	-5.433645	-2.304054	-7.567307	Cd	-12.294446	-2.333221	-12.895428
H	-8.659213	0.460200	-6.900006	Cd	-12.077108	-3.764037	-19.154346
H	-9.536730	0.000969	-9.158360	Cd	-14.285974	-7.778506	-15.076942
H	-6.311179	-2.763668	-9.825687	Cd	-12.086515	-4.988271	-15.639790

11.2. Cd₁₃Se₁₃-BTT-Cd₁₃Se₁₃

C	-3.656049	-0.506096	-5.543027	Cd	-4.518487	2.361717	-0.447881
C	-2.341288	-0.352182	-5.081826	Cd	-5.431680	-2.189485	-3.318801
C	-1.752292	0.900214	-4.905811	Cd	-8.885332	3.108637	-0.517482
C	-2.442323	2.091767	-5.248766	Cd	-6.994861	1.159930	-3.579360
C	-3.751764	1.932227	-5.737793	Se	2.926656	8.898256	-0.927778
C	-4.356191	0.681178	-5.854706	Se	3.257458	8.758355	3.901224
H	-1.781573	-1.243882	-4.819515	Se	-0.696208	10.811669	1.869013
H	-4.314695	2.829181	-5.980242	Cd	3.347092	7.583883	1.342550
S	-1.771421	3.727773	-5.128360	Cd	0.298593	9.499302	-0.218124
S	-0.143801	0.924636	-4.103054	Cd	0.634835	9.219111	3.697662
S	-6.113474	0.660320	-6.254228	Cd	1.472141	6.876708	-2.090114
S	-4.378203	-2.141959	-5.641698	Cd	-2.536528	8.876512	2.588435
Se	-5.841876	-2.447409	4.165321	Cd	2.819287	6.122136	4.266801
Se	-8.812831	-4.816367	1.020981	Se	-0.958245	8.087095	-2.231319
Se	-10.757543	-1.295674	3.887144	Se	-1.554751	8.221333	5.045789
Cd	-6.546555	-3.493965	1.867571	Se	3.992762	4.980815	2.053862
Cd	-8.146282	-0.911779	4.278025	Se	1.937537	4.252109	-2.185386
Cd	-10.364805	-2.677774	1.554306	Se	1.143274	4.611453	5.762185
Cd	-4.853331	0.165297	3.553154	Se	-4.223037	7.586248	0.981509
Cd	-11.049941	0.594685	1.846269	Cd	1.742588	4.225319	0.553295
Cd	-7.924368	-3.742199	-1.272754	Cd	-1.029142	5.703162	4.162288
Se	-6.837872	1.468219	4.849999	Cd	-1.952188	6.513910	-0.263866
Se	-11.786726	-1.115143	-0.193325	Se	0.139746	6.310653	1.631752
Se	-5.171690	-3.562169	-0.753360	Se	1.000220	1.698281	1.616980
Se	-3.382290	0.352407	1.375402	Se	-2.245875	3.810601	-0.675324
Se	-8.270583	-2.141873	-3.374097	Se	-2.927522	3.730099	3.773372
Se	-10.270215	3.145132	1.803547	Cd	-0.598414	3.560278	-2.835787
Cd	-5.336474	-0.873242	-0.124811	Cd	1.492794	2.885582	3.854339
Cd	-9.515844	-0.439778	-1.515752	Cd	-4.440348	5.219135	2.158634
Cd	-7.673028	2.302153	2.467860	Cd	-1.569753	2.566127	1.701075
Se	-7.808103	-0.277172	0.820374	H	0.487329	1.732721	-4.987240
Se	-4.699019	0.529101	-2.467829	H	-6.194682	-0.703655	-6.17122
Se	-6.431392	3.917891	0.602509				
Se	-9.386101	2.046712	-2.901783				

11.3. Cd₁₇Se₄(SCH₃)₂₆-Py-Py- Cd₁₇Se₄(S CH₃)₂₆

Cd	-11.954547	0.011980	-0.056096	H	-16.804631	-5.330508	7.967082
Cd	-11.585494	-1.210209	-4.307209	H	-15.352724	-5.578175	6.978814
Cd	-14.057713	-4.538205	-4.580706	H	-16.739235	-4.698312	6.309149
Cd	-5.999809	0.486227	-0.150348	S	-12.016952	-3.083651	5.506732
Cd	-8.862286	1.537162	-2.727261	C	-12.336793	-4.880451	5.820711
Cd	-8.599848	-2.374252	-0.126140	H	-12.840194	-5.350646	4.972866
Cd	-12.027449	-4.424904	-0.894288	H	-12.969317	-4.953359	6.709439
Cd	-15.172405	-1.266125	-2.288815	H	-11.388463	-5.391520	6.001331
Se	-9.283866	0.287178	-0.297837	S	-12.261288	-5.003660	1.658840
Se	-12.554160	-1.886844	-1.822261	C	-14.073327	-5.159921	1.980486
Cd	-12.656517	2.804627	-3.255506	H	-14.474204	-5.968856	1.366354
Cd	-12.460742	1.050203	4.390271	H	-14.604354	-4.237486	1.742760
Cd	-14.533522	-2.244782	5.841627	H	-14.240250	-5.390874	3.034555
Cd	-14.220874	5.599867	-0.948579	S	-16.616707	-2.447998	-0.464443
Cd	-11.573218	3.906218	1.506715	C	-15.971878	-4.157936	-0.721653
Cd	-15.558027	2.100576	0.092825	H	-16.395335	-4.825709	0.030391
Cd	-15.733950	-1.507349	1.831325	H	-14.883278	-4.182218	-0.651980
Cd	-11.714167	-2.840312	2.965510	H	-16.261964	-4.507339	-1.715415
Se	-12.891442	2.500866	-0.491196	S	-15.608721	-2.371275	-4.570303
Se	-13.133601	-0.614245	2.268503	C	-17.276775	-3.162699	-4.402060
Cd	-8.883267	0.801917	2.516135	H	-17.546040	-3.292472	-3.350487
C	-16.198331	8.226970	-0.394459	H	-17.245548	-4.135496	-4.900768
C	-16.816367	9.467306	-0.534913	H	-18.022068	-2.526201	-4.885403
C	-16.525793	10.235227	-1.663792	S	-15.246183	-6.046645	-6.205950
C	-15.630771	9.734120	-2.609930	C	-14.907361	-7.718835	-5.489611
C	-15.056120	8.483870	-2.390574	H	-15.655584	-8.419259	-5.873155
N	-15.332503	7.744140	-1.302840	H	-14.971203	-7.711765	-4.397084
H	-16.395722	7.580226	0.456532	H	-13.916830	-8.081450	-5.784151
H	-17.509302	9.816658	0.223534	S	-13.366870	-5.990583	-2.429523
H	-15.379619	10.295962	-3.503578	C	-12.004509	-6.945849	-3.248481
H	-14.360279	8.039472	-3.097227	H	-12.454866	-7.757237	-3.824083
C	-2.869225	0.419145	1.069984	H	-11.341928	-7.368014	-2.488757
C	-1.479480	0.407758	1.126690	H	-11.432053	-6.304977	-3.923752
C	-0.741096	0.780944	-0.006667	S	-9.402771	-4.676287	-0.939723
C	-1.459691	1.149433	-1.153811	C	-8.976701	-4.722867	-2.739252
C	-2.850352	1.129198	-1.125194	H	-7.932948	-4.430251	-2.872261
N	-3.548076	0.774191	-0.033754	H	-9.620151	-4.065995	-3.327328
H	-3.476902	0.128533	1.922713	H	-9.108977	-5.748523	-3.089468
H	-0.982933	0.084921	2.035746	S	-6.033286	-2.093278	-0.696221
H	-0.947757	1.467836	-2.055826	C	-5.208931	-2.785688	0.810550
H	-3.442345	1.395677	-1.996729	H	-5.412317	-3.857843	0.869959
S	-15.483753	-3.293565	7.921843	H	-5.562815	-2.295639	1.720599
C	-16.153767	-4.870628	7.217369	H	-4.128889	-2.636869	0.725896

S	-9.089033	3.477186	2.132036	S	-11.700736	-3.549017	-5.383268
C	-8.115891	3.720660	0.592149	C	-12.151453	-3.251212	-7.155618
H	-8.514983	3.124352	-0.229782	H	-12.434598	-4.207911	-7.600785
H	-7.083924	3.403419	0.773026	H	-11.292885	-2.833647	-7.686866
H	-8.118676	4.777974	0.317891	H	-12.999730	-2.566578	-7.231620
S	-6.210058	1.764039	-2.413555	S	-9.201575	-2.090762	2.458899
C	-5.873035	3.562085	-2.164114	C	-8.115657	-3.090574	3.564688
H	-5.910591	4.054898	-3.138579	H	-8.602949	-3.215178	4.534326
H	-4.874217	3.695932	-1.738193	H	-7.167539	-2.564046	3.697073
H	-6.605753	4.028845	-1.504559	H	-7.936923	-4.071899	3.119894
S	-6.225079	0.543832	2.455974	S	-9.912338	1.075875	4.912968
C	-5.601598	2.181404	3.046997	C	-9.498002	-0.497219	5.780940
H	-6.353895	2.960895	2.908849	H	-8.412978	-0.552789	5.901392
H	-4.686792	2.450816	2.510892	H	-9.848405	-1.365222	5.225696
H	-5.377413	2.101020	4.113308	H	-9.970652	-0.500602	6.765325
S	-12.186712	6.305688	0.514459	S	-14.465892	0.413312	5.880441
C	-13.021961	7.120119	1.952143	C	-13.921737	0.675463	7.630830
H	-12.256336	7.506345	2.628600	H	-14.702513	0.296207	8.294360
H	-13.650570	6.415799	2.500939	H	-13.776790	1.743202	7.812189
H	-13.632867	7.952589	1.592479	H	-12.991578	0.140513	7.836833
S	-16.287091	4.647237	0.356155	S	-12.760412	3.616335	3.799468
C	-17.633135	4.754126	-0.909589	C	-14.546283	3.523104	3.355639
H	-18.568908	4.419731	-0.455433	H	-14.878066	4.446751	2.876749
H	-17.409755	4.125710	-1.774396	H	-15.125441	3.361447	4.266520
H	-17.746432	5.790527	-1.239600	H	-14.732877	2.683647	2.680953
S	-13.885044	5.138906	-3.494966	S	-17.165498	0.692723	1.537527
C	-15.601318	4.733034	-4.057573	C	-17.253594	1.481952	3.206262
H	-15.944010	3.793005	-3.620371	H	-17.324175	2.566246	3.093299
H	-15.594437	4.640512	-5.146372	H	-16.385878	1.234394	3.820264
H	-16.280024	5.542220	-3.774834	H	-18.155811	1.115618	3.701538
S	-15.974303	1.249350	-2.348632	H	-16.990867	11.206698	-1.804534
C	-17.785242	0.873389	-2.464902	S	-10.138560	3.659501	-3.446264
H	-17.969524	0.286779	-3.368547	C	-10.119566	4.839005	-2.029022
H	-18.345818	1.809629	-2.522531	H	-10.816585	5.653950	-2.239714
H	-18.115998	0.307350	-1.591260	H	-9.118780	5.257171	-1.903387
S	-12.692239	1.038031	-5.128717	H	-10.425259	4.349515	-1.103493
C	-14.423387	0.813064	-5.729005	S	-16.199904	-2.985647	3.881203
H	-14.704391	1.702471	-6.298776	C	-17.677561	-2.168086	4.648142
H	-15.117921	0.668311	-4.902785	H	-17.815970	-2.589318	5.647192
H	-14.458826	-0.062978	-6.378393	H	-18.561278	-2.362696	4.036164
S	-9.140740	-0.249428	-4.576359	H	-17.524824	-1.090801	4.744275
C	-8.064185	-1.562494	-3.855203	Cd	11.954554	0.011967	0.056079
H	-7.044453	-1.184155	-3.745743	Cd	11.585328	-1.210199	4.307187
H	-8.059168	-2.427534	-4.520854	Cd	14.057413	-4.538235	4.580797
H	-8.430410	-1.874818	-2.874680	Cd	5.999798	0.486285	0.150061

Cd	8.862180	1.537155	2.727129	H	12.969619	-4.953338	-6.709415
Cd	8.599823	-2.374226	0.125954	H	11.388706	-5.391484	-6.001428
Cd	12.027362	-4.424900	0.894266	S	12.261363	-5.003651	-1.658849
Cd	15.172297	-1.266141	2.288968	C	14.073426	-5.159843	-1.980392
Se	9.283864	0.287197	0.297700	H	14.474291	-5.968790	-1.366269
Se	12.554076	-1.886851	1.822266	H	14.604406	-4.237400	-1.742591
Cd	12.656390	2.804617	3.255526	H	14.240421	-5.390744	-3.034461
Cd	12.460966	1.050202	-4.390263	S	16.616662	-2.448046	0.464657
Cd	14.533784	-2.244803	-5.841493	C	15.971773	-4.157968	0.721824
Cd	14.220877	5.599850	0.948683	H	16.395260	-4.825752	-0.030194
Cd	11.573326	3.906203	-1.506730	H	14.883175	-4.182222	0.652081
Cd	15.558061	2.100550	-0.092658	H	16.261786	-4.507380	1.715604
Cd	15.734025	-1.507358	-1.831155	S	15.608431	-2.371311	4.570485
Cd	11.714268	-2.840306	-2.965545	C	17.276490	-3.162749	4.402362
Se	12.891453	2.500847	0.491234	H	17.545827	-3.292531	3.350809
Se	13.133701	-0.614256	-2.268473	H	17.245222	-4.135542	4.901075
Cd	8.883391	0.801942	-2.516295	H	18.021756	-2.526255	4.885752
C	16.198389	8.226930	0.394652	S	15.245770	-6.046684	6.206116
C	16.816424	9.467263	0.535130	C	14.906880	-7.718877	5.489817
C	16.525795	10.235195	1.663987	H	15.655091	-8.419316	5.873357
C	15.630719	9.734101	2.610081	H	14.970695	-7.711830	4.397289
C	15.056071	8.483853	2.390703	H	13.916345	-8.081457	5.784388
N	15.332508	7.744113	1.302989	S	13.366691	-5.990603	2.429562
H	16.395824	7.580178	-0.456323	C	12.004279	-6.945873	3.248427
H	17.509402	9.816605	-0.223282	H	12.454601	-7.757242	3.824083
H	15.379521	10.295950	3.503711	H	11.341768	-7.368063	2.488656
H	14.360188	8.039466	3.097322	H	11.431757	-6.304996	3.923637
C	2.869186	0.419331	-1.070286	S	9.402685	-4.676286	0.939511
C	1.479442	0.407968	-1.126975	C	8.976457	-4.722935	2.739000
C	0.741080	0.780984	0.006467	H	7.932701	-4.430293	2.871931
C	1.459709	1.149401	1.153611	H	9.619876	-4.066109	3.327160
C	2.850372	1.129162	1.124972	H	9.108670	-5.748612	3.089181
N	3.548052	0.774250	0.033472	S	6.033245	-2.093241	0.695901
H	3.476845	0.128824	-1.923067	C	5.208957	-2.785598	-0.810934
H	0.982837	0.085308	-2.036061	H	5.412308	-3.857759	-0.870343
H	0.947801	1.467775	2.055653	H	5.562912	-2.295545	-1.720950
H	3.442404	1.395567	1.996501	H	4.128915	-2.636741	-0.726341
S	15.484055	-3.293596	-7.921683	S	9.089162	3.477201	-2.132174
C	16.154133	-4.870613	-7.217167	C	8.115934	3.720651	-0.592337
H	16.805011	-5.330489	-7.966869	H	8.514963	3.124302	0.229595
H	15.353117	-5.578184	-6.978588	H	7.083968	3.403445	-0.773280
H	16.739596	-4.698247	-6.308954	H	8.118732	4.777956	-0.318045
S	12.017199	-3.083632	-5.506753	S	6.209984	1.764068	2.413317
C	12.337031	-4.880433	-5.820732	C	5.873018	3.562131	2.163916
H	12.840363	-5.350651	-4.972858	H	5.910592	4.054918	3.138394

H	4.874204	3.696019	1.738000	H	12.433980	-4.208052	7.600742
H	6.605752	4.028880	1.504373	H	11.292276	-2.833775	7.686751
S	6.225202	0.543881	-2.456249	H	12.999178	-2.566710	7.231718
C	5.601689	2.181426	-3.047290	S	9.201665	-2.090737	-2.459043
H	6.353883	2.960986	-2.908967	C	8.115776	-3.090526	-3.564880
H	4.686761	2.450726	-2.511337	H	8.603093	-3.215112	-4.534508
H	5.377712	2.101091	-4.113647	H	7.167663	-2.563996	-3.697282
S	12.186791	6.305681	-0.514459	H	7.937031	-4.071861	-3.120110
C	13.022106	7.120108	-1.952105	S	9.912577	1.075890	-4.913085
H	12.256512	7.506340	-2.628595	C	9.498267	-0.497206	-5.781068
H	13.650735	6.415786	-2.500876	H	8.413248	-0.552769	-5.901566
H	13.633001	7.952576	-1.592415	H	9.848641	-1.365208	-5.225806
S	16.287156	4.647207	-0.355941	H	9.970958	-0.500597	-6.765434
C	17.633132	4.754075	0.909877	S	14.466198	0.413292	-5.880317
H	18.568930	4.419690	0.455765	C	13.922142	0.675441	-7.630738
H	17.409707	4.125643	1.774660	H	14.702948	0.296169	-8.294224
H	17.746410	5.790470	1.239914	H	13.777220	1.743181	-7.812112
S	13.884920	5.138887	3.495052	H	12.991986	0.140503	-7.836788
C	15.601166	4.732982	4.057727	S	12.760609	3.616323	-3.799434
H	15.943867	3.792960	3.620518	C	14.546460	3.523091	-3.355524
H	15.594235	4.640437	5.146523	H	14.878215	4.446729	-2.876598
H	16.279894	5.542167	3.775035	H	15.125661	3.361459	-4.266383
S	15.974229	1.249314	2.348819	H	14.733028	2.683617	-2.680851
C	17.785161	0.873331	2.465139	S	17.165588	0.692691	-1.537278
H	17.969413	0.286714	3.368785	C	17.253823	1.481919	-3.206005
H	18.345744	1.809565	2.522791	H	17.324414	2.566212	-3.093035
H	18.115935	0.307294	1.591502	H	16.386149	1.234376	-3.820073
S	12.692091	1.038016	5.128744	H	18.156071	1.115568	-3.701211
C	14.423235	0.813030	5.729035	H	16.990868	11.206664	1.804747
H	14.704238	1.702423	6.298829	S	10.138426	3.659491	3.446176
H	15.117771	0.668295	4.902813	C	10.119484	4.838969	2.028909
H	14.458670	-0.063029	6.378400	H	10.816502	5.653914	2.239602
S	9.140570	-0.249399	4.576266	H	9.118703	5.257141	1.903245
C	8.064069	-1.562512	3.855115	H	10.425195	4.349459	1.103398
H	7.044324	-1.184210	3.745645	S	16.200093	-2.985652	-3.881003
H	8.059083	-2.427544	4.520775	C	17.677766	-2.168068	-4.647886
H	8.430311	-1.874829	2.874595	H	17.816250	-2.589333	-5.646911
S	11.700389	-3.549046	5.383168	H	18.561455	-2.362621	-4.035850
C	12.150901	-3.251329	7.155585	H	17.524994	-1.090792	-4.744071

12. References

1. Behrens, S.; Marco, B.; Eichhfer, A.; Fenske, D., Synthesis and Crystal Structure of Cd₁₀Se(SePh)₁₂(PPh₃)₄ and Cd₁₆(SePh)₃₂(PPh₃)₂. *Angewandte Chemie International Edition* **1997**, *36* (24), 2797--2799.
2. Soloviev, V. N.; Eichhofer, A.; Fenske, D.; Banin, U., Molecular limit of a bulk semiconductor: Size dependence of the 'band gap' in CdSe cluster molecules 15. *Journal of the American Chemical Society* **2000**, *122* (11), 2673--2674.
3. Yu, H. S.; He, X.; Li, S. L.; Truhlar, D. G., MN15: A Kohn–Sham global-hybrid exchange–correlation density functional with broad accuracy for multi-reference and single-reference systems and noncovalent interactions. *Chemical Science* **2016**, *7* (8), 5032-5051.
4. Yanai, T.; Tew, D. P.; Handy, N. C., A new hybrid exchange–correlation functional using the Coulomb-attenuating method (CAM-B3LYP). *Chemical Physics Letters* **2004**, *393* (1), 51-57.
5. Luzanov, A. V., Excited State Structural Analysis: TDDFT and Related Models. **2012**, 415--449.
6. Plasser, F.; Lischka, H., Analysis of Excitonic and Charge Transfer Interactions from Quantum Chemical Calculations. *Journal of Chemical Theory and Computation* **2012**, *8* (8), 2777--2789.
7. Plasser, F. W., Michael; Dreuw, A., New tools for the systematic analysis and visualization of electronic excitations. I. Formalism. *J. Chem. Phys.* **2014**, *141*, 024106.